

Compression for 2-Parameter Persistent Homology^{*}

Ulderico Fugacci[†] Michael Kerber[‡] Alexander Rolle[‡]

Abstract

Compression aims to reduce the size of an input, while maintaining its relevant properties. For multi-parameter persistent homology, compression is a necessary step in any computational pipeline, since standard constructions lead to large inputs, and computational tasks in this area tend to be expensive. We propose two compression methods for chain complexes of free 2-parameter persistence modules. The first method extends the multi-chunk algorithm for one-parameter persistent homology, returning the smallest chain complex among all the ones quasi-isomorphic to the input. The second method produces minimal presentations of the homology of the input; it is based on an algorithm of Lesnick and Wright, but incorporates several improvements that lead to substantial performance gains. The two methods are complementary, and can be combined to compute minimal presentations for complexes with millions of generators in a few seconds. The methods have been implemented, and the software is publicly available. We report on experimental evaluations, which demonstrate substantial improvements in performance compared to previously available compression strategies.

1 Introduction

Motivation Persistent homology is a powerful tool in data analysis enabling the characterization and the comparison of a large variety of datasets on the basis of their topological properties. Specifically, the typical pipeline of persistent homology assigns to each data set a filtered simplicial complex evolving along a real-valued parameter. Then, persistent homology describes and discriminates data by studying the birth and the death of the topological features (such as connected components, loops, tunnels, and so on) occurring during the filtration.

While this strategy has proven its effectiveness in several scenarios, it is quite common in applications to face datasets that are parametrized through multiple scalar functions. This naturally calls for the development of a multi-parameter

^{*}This work was supported by the Austrian Science Fund (FWF) grant numbers P 29984-N35 and P 33765-N.

[†]Istituto di Matematica Applicata e Tecnologie Informatiche “E. Magenes”, Consiglio Nazionale delle Ricerche, Italy

[‡]Graz University of Technology, Austria

extension of persistent homology. Despite its potential, multi-parameter persistent homology has not found as widespread distribution as the one-parameter case: a major obstruction is the impossibility of summarizing the topological information by a complete and discrete invariant such as the barcode in the one-parameter setting [1] (which encodes the births and deaths mentioned above). Still, recent work has proposed algorithmic solutions to visualize multi-parameter persistence modules [2], to compare them via the matching distance [3, 4, 5], the bottleneck distance [6] or via kernels [7, 8], and to decompose them into indecomposable summands [9]. What is common to these approaches is that the computation tends to be expensive. For instance, the algorithm to compute the matching distance has expected running time $O(n^5 \log^3 n)$ for 2-parameters, where the worst-case complexity for a single parameter is only $O(n^{1.5} \log n)$ [10]. So despite all efforts, distance computations in the 2-parameter case must be restricted in practice to modules of moderate size.

By **compression** of a representation of a multi-parameter topological object (e.g. a filtered simplicial complex, filtered chain complex, or a persistence module) we mean replacing the representation with a smaller representation such that the relevant topological properties are preserved. Computations on compressed representations yield the same outcome by definition, and will perform faster because of the reduced input size. Hence, compression has the potential to improve the performance of each of the aforementioned approaches. We therefore consider compression as an indispensable pre-processing step of the computational pipeline of multi-parameter topological data analysis.

Contribution This paper proposes two compression algorithms for 2-parameter persistent homology. Both algorithms take as input chain complexes of free 2-parameter persistence modules; as an example, bi-filtered simplicial complexes naturally yield such chain complexes with simplices as free generators (see Example 2.6). Both our approaches return a structure that is minimal in an appropriate sense, but they differ in how much topological information they preserve.

The first approach, called **multi-chunk**, computes another chain complex of free 2-parameter persistence modules with the property that it is the smallest such chain complex among all those quasi-isomorphic to the input. The algorithm is an extension of the *chunk* algorithm for one-parameter persistent homology [11]: it proceeds by first identifying pairs of generators in consecutive dimensions that do not contribute to the homology of the complex, and then changing the boundaries of the generators to remove all those pairs. Both steps can be performed quickly in practice using similar speed-ups as in the one-parameter counterpart. Moreover, both steps can easily be parallelized with shared-memory.

The second approach, called **mpfree**, computes a *minimal presentation matrix* for the homology of the chain complex in a chosen degree. A presentation matrix encodes the generators and relations of a module. It is minimal if the total numbers of generators and relations is minimal. A minimal presentation

of the homology is typically smaller than the chain complex produced by multi-chunk, with the price that the chain complex structure is lost. Some important algorithms in multi-parameter persistence require a presentation as input [12, 9], and this is further motivation for computing minimal presentations efficiently.

Our algorithm `mpfree` is an improved version of the pioneering work of Lesnick and Wright [12] which arrives at a minimal presentation matrix through column additions. Our improvements stem from two major observations: first, their algorithm often spends more time in *looking* for the next column addition to be performed than it does in *performing* the addition. We show that the necessary column operations can be predicted from previous steps, and we maintain this information in priority queues to avoid linear scans. Second, we observe that the last step of the algorithm (which turns a so-called semi-minimal presentation into a minimal one) can be done more efficiently using `multi-chunk`.

Both approaches have been implemented in C++ and the software is publicly available [13, 14]. We extensively benchmark our implementations on a variety of data sets including triangular mesh data, bi-filtered flag complexes and others. We show that computing minimal chain complexes and minimal presentations scales linearly in terms of time and memory size in practice and is possible for complexes with millions of simplices within seconds. In particular, our improvements lead to a significant improvement over the RIVET library [15], which implements the algorithm by Lesnick and Wright. Moreover, the resulting compressed outputs are significantly smaller than the input and thus result in a satisfying compression rate.

We also show that `multi-chunk` generally performs faster than `mpfree`, and its running time is dominated by reading the input file. More speed-ups can be achieved by first calling `multi-chunk`, followed by `mpfree` on the compressed chain complex. Partially, the advantage of that strategy comes from the *clearing optimization* [16, 11] that avoids some operations in dimension d through the information obtained in dimension $d + 1$. Since minimal presentations focus on a single dimension, the advantage of clearing is mostly lost when using `mpfree` alone.

Our experiments also show a (modest) advantage of parallelization, and we investigate the running time of the major subroutines of our algorithm. Finally, we report on a perhaps counter-intuitive observation that the algorithm is sometimes faster when applied to a chain complex $C_3 \rightarrow C_2 \rightarrow C_1 \rightarrow C_0 \rightarrow 0$ than when only applied to the sub-complex $C_2 \rightarrow C_1 \rightarrow C_0$.

Differences to the conference versions Both presented approaches appeared as prior conference papers; see [17] for `multi-chunk` and [18] for `mpfree`. We think that because both approaches share the goal of compression and also are symbiotic on a mathematical and implementation level, it is natural to present them together in this journal version. Furthermore, in the conference versions, the two algorithms were described using different frameworks; in this paper we describe the two algorithms within the same framework (both take as input chain complexes of free, multi-parameter persistence modules). By

unifying the language, we clarify the relationship between the two algorithms. Notably, we can describe one sub-routine of `mpfree` (the minimization) as an instance of `multi-chunk`, which was not clear in the conference version. We also provide a new complexity analysis for `mpfree`, which sheds light on the improvement in performance over RIVET that we observe in the experiments. Moreover, we provide proof details that had to be skipped in the conference version because of size limits. Finally, this paper contains experimental evaluation for new benchmark instances and investigates the interplay of both algorithms in the case of “long” chain complexes.

Related work Compression has been studied extensively for the one-parameter case in the context of persistence computation. Besides the aforementioned chunk algorithm [11], several papers propose the use of discrete Morse theory to collapse pairs of simplices without changing the homotopy type, reducing the size of the considered boundary matrix [19, 20]. Also, the efficiency of state-of-the-art software for flag complexes, such as Ripser [21] and Eirene [22] is to a large extent due to implicit compression. Another recent line of research uses the concept of strong collapses to arrive at a small complex quickly, in general [23], and for flag complexes [24].

All the above approaches are examples of *lossless compression*, in the sense that the compressed complex has an equivalent persistence diagram to the input. Better compression rates are possible with *lossy compression*. Here, it is only guaranteed that the compressed complex has a persistence diagram that is close to the input. This idea has been extensively studied in theory [25, 26, 27, 28, 29] and practice [30, 31, 32].

In the multi-parameter case, one line of research lifts the idea of discrete Morse collapses to the multi-parameter case [33, 34, 35, 36]. Our `multi-chunk` algorithm is motivated by this line of research and attempts to compress the complex on the level of persistence computation directly instead of using discrete Morse theory. This leads to a provably minimal chain complex which can be guaranteed in the aforementioned approach only for special cases. We point out, however, that the related work returns a Forman gradient together with the cell complex, and applications might profit from this additional structure. Finally, we compared our `multi-chunk` algorithm with the approach in [35]: `multi-chunk` is faster, and both approaches have comparable memory consumption and produce compressions of similar size in practice. We refer to the the conference version of `multi-chunk` [17] for more details on this comparison.

Minimal presentations can be computed for more general (graded) modules, and general algorithms are provided by computer algebra systems like Macaulay or Singular. Lesnick and Wright [2] compare their implementation with these systems and show that their algorithm is much faster for the special case of chain complexes of free 2-parameter persistence modules.

Outline The remainder of this paper is organized as follows. In Section 2 we introduce the required background notions. In Section 3 we describe

`multi-chunk`, while in Section 4 we describe `mpfree`. In more detail, Section 3.1 discusses the input and output settings of `multi-chunk`, Section 3.2 describes the details of the algorithm, while Sections 3.3, 3.4, and 3.5 focus on the correctness, the complexity, and the optimality of `multi-chunk`, respectively. Similarly, Section 4.1 discusses the input and output settings of `mpfree`, Section 4.2 describes the algorithm of Lesnick and Wright on which `mpfree` is based, Sections 4.3 and 4.4 focus on our improvements, while Section 4.5 analyses the complexity of `mpfree`. In Section 5 we present and discuss the experimental results. Finally, in Section 6, we summarize our contributions and we draw some conclusions. A contains proof details, and B contains pseudocode.

2 Definitions

This section presents standard definitions and facts about multi-parameter persistence modules. For more details, see [1, 12]. Fix a field k . All vector spaces in this section will be over k . Let $d \geq 1$ be a natural number.

Definition 2.1. Let \mathbb{Z}^d be the poset with $(w_1, \dots, w_d) \leq (z_1, \dots, z_d)$ if $w_i \leq z_i$ for all $1 \leq i \leq d$. A d -parameter **persistence module** is a functor $M : \mathbb{Z}^d \rightarrow \text{Vec}$ from the poset \mathbb{Z}^d to the category of vector spaces over k . A **homomorphism of persistence modules** is a natural transformation. For $\mathbf{z} \in \mathbb{Z}^d$ we write $M_{\mathbf{z}} = M(\mathbf{z})$, and for $\mathbf{w} \leq \mathbf{z}$ in \mathbb{Z}^d we write $M_{\mathbf{w}, \mathbf{z}} = M(\mathbf{w} \leq \mathbf{z}) : M_{\mathbf{w}} \rightarrow M_{\mathbf{z}}$.

The category of persistence modules is an abelian category, because it is a category of functors valued in an abelian category [37, 8.3.6]. So, we can form direct sums, kernels, and cokernels, and these are computed “pointwise”. For example, the kernel of a homomorphism $f : M \rightarrow N$ of d -parameter persistence modules is the persistence module $\text{Ker}(f)$ with $\text{Ker}(f)_{\mathbf{z}} = \text{Ker}(f_{\mathbf{z}} : M_{\mathbf{z}} \rightarrow N_{\mathbf{z}})$ for all $\mathbf{z} \in \mathbb{Z}^d$, and with the induced homomorphisms $\text{Ker}(f)_{\mathbf{w}, \mathbf{z}} : \text{Ker}(f)_{\mathbf{w}} \rightarrow \text{Ker}(f)_{\mathbf{z}}$.

The term “persistence module” comes from the following alternative definition:

Remark 2.2. Equivalently, a d -parameter persistence module is a module M over the polynomial ring $k[x_1, \dots, x_d]$ equipped with a \mathbb{Z}^d -grading, which is a vector space decomposition $M = \bigoplus_{\mathbf{z} \in \mathbb{Z}^d} M_{\mathbf{z}}$ such that $x_i \cdot M_{\mathbf{z}} \subseteq M_{\mathbf{z} + \mathbf{e}_i}$ for all $\mathbf{z} \in \mathbb{Z}^d$, where \mathbf{e}_i is the i^{th} standard basis vector. An element v of M such that $v \in M_{\mathbf{z}}$ for some $\mathbf{z} \in \mathbb{Z}^d$ is called homogenous. In this language, a homomorphism $f : M \rightarrow N$ of persistence modules is a module homomorphism such that $f(M_{\mathbf{z}}) \subseteq N_{\mathbf{z}}$ for all $\mathbf{z} \in \mathbb{Z}^d$.

If $M : \mathbb{Z}^d \rightarrow \text{Vec}$ is a persistence module, and $v \in M_{\mathbf{z}}$ for some $\mathbf{z} \in \mathbb{Z}^d$, we say that \mathbf{z} is the **grade** of v , and we write $\text{gr}(v) = \mathbf{z}$. In the language of Remark 2.2, only the homogenous elements have a grade.

A standard way to understand persistence modules is to represent them using homomorphisms between persistence modules with a simple form. These are the free persistence modules:

Definition 2.3. For $\mathbf{u} \in \mathbb{Z}^d$, let $E^{\mathbf{u}}$ be the d -parameter persistence module with

$$E_{\mathbf{z}}^{\mathbf{u}} = \begin{cases} k & \text{if } \mathbf{u} \leq \mathbf{z} \\ 0 & \text{else} \end{cases} \quad \text{and} \quad E_{\mathbf{w}, \mathbf{z}}^{\mathbf{u}} = \begin{cases} \text{id} & \text{if } \mathbf{u} \leq \mathbf{w} \\ 0 & \text{else} \end{cases}.$$

A d -parameter persistence module F is **free** if there is a multiset G of elements in \mathbb{Z}^d such that $F \cong \bigoplus_{\mathbf{u} \in G} E^{\mathbf{u}}$. Using the language of Remark 2.2, a **basis** for a free persistence module F is a minimal homogenous set of generators for F .

It follows from a graded version of Nakayama's lemma [38, Corollary 4.8] that the number of elements at each grade in a basis of a free persistence module is an isomorphism invariant.

The input to the algorithms of this paper will be chain complexes of free persistence modules, which we now define. Because we use subscripts for grades, we will use superscripts for the dimension of a persistence module in a chain complex; note that this is contrary to the usual convention of using subscripts for the dimension. Because cohomology will not appear in this paper, this should not cause confusion.

Definition 2.4. A **chain complex** of free persistence modules F^\bullet is a diagram of the form

$$\dots \xrightarrow{\partial^3} F^2 \xrightarrow{\partial^2} F^1 \xrightarrow{\partial^1} F^0$$

where each F^i is a free d -parameter persistence module, and $\partial^i \circ \partial^{i+1} = 0$ for all $i \geq 1$. If F^\bullet and G^\bullet are chain complexes of free persistence modules, then a **chain map** $f^\bullet : F^\bullet \rightarrow G^\bullet$ consists of homomorphisms $f^i : F^i \rightarrow G^i$ for all $i \geq 0$, such that the following diagram commutes for all $i \geq 0$:

$$\begin{array}{ccc} F^{i+1} & \xrightarrow{f^{i+1}} & G^{i+1} \\ \partial^{i+1} \downarrow & & \downarrow \partial^{i+1} \\ F^i & \xrightarrow{f^i} & G^i \end{array}$$

The homology of a chain complex of free persistence modules is defined in the usual way:

Definition 2.5. Let F^\bullet be a chain complex of free persistence modules. For $n \geq 0$, the **homology** $H^n(F^\bullet)$ is the d -parameter persistence module $\text{Ker}(\partial^n)/\text{Im}(\partial^{n+1})$. If $f^\bullet : F^\bullet \rightarrow G^\bullet$ is a chain map, then there are induced homomorphisms $f_*^n : H^n(F^\bullet) \rightarrow H^n(G^\bullet)$.

Example 2.6. A d -parameter filtered simplicial complex is a functor $S : \mathbb{Z}^d \rightarrow \text{SimpComplex}$ valued in the category of simplicial complexes, such that for all $\mathbf{w} \leq \mathbf{z}$ in \mathbb{Z}^d , the map $S_{\mathbf{w}} \rightarrow S_{\mathbf{z}}$ is an inclusion. Let $C : \text{SimpComplex} \rightarrow \text{ChComplex}$ be the oriented chain complex functor, so that the simplicial homology of a simplicial complex L is the homology of the chain complex $C(L)$.

Composing S with C we get a functor $CS : \mathbb{Z}^d \rightarrow \text{ChComplex}$. In particular, for each $i \geq 0$ we have a persistence module $CS^i : \mathbb{Z}^d \rightarrow \text{Vec}$ where $CS_{\mathbf{z}}^i$ is the i^{th} degree part of $CS_{\mathbf{z}}$. If each CS^i is free, then the filtered simplicial complex S is called “one-critical”, and we have a chain complex of free persistence modules $\cdots CS^2 \rightarrow CS^1 \rightarrow CS^0$. Such filtered simplicial complexes are the main source of examples for this paper.

Definition 2.7. Let F^\bullet and G^\bullet be chain complexes of free persistence modules. F^\bullet and G^\bullet are **isomorphic** if there exist chain maps $f^\bullet : F^\bullet \rightarrow G^\bullet$ and $g^\bullet : G^\bullet \rightarrow F^\bullet$ such that $g \circ f = \text{id}_{F^\bullet}$ and $f \circ g = \text{id}_{G^\bullet}$.

Definition 2.8. Let F^\bullet and G^\bullet be chain complexes of free persistence modules. We say that F^\bullet and G^\bullet are **homology equivalent** if for all $n \geq 0$ there is an isomorphism $H^n(F^\bullet) \cong H^n(G^\bullet)$. We say that F^\bullet and G^\bullet are **quasi-isomorphic** if there is a chain map $f : F^\bullet \rightarrow G^\bullet$ such that all induced homomorphisms $f_*^n : H^n(F^\bullet) \rightarrow H^n(G^\bullet)$ are isomorphisms.

An important class of quasi-isomorphisms are the homotopy equivalences:

Definition 2.9. Let F^\bullet and G^\bullet be chain complexes of free persistence modules. If $f, g : F^\bullet \rightarrow G^\bullet$ are chain maps, then we say that f and g are **chain-homotopic** if there are homomorphisms $h^n : F^n \rightarrow G^{n+1}$ such that $\partial^{n+1} \circ h^n + h^{n-1} \partial^n = f^n - g^n$ for all $n \geq 0$. We say that F^\bullet and G^\bullet are **homotopy equivalent** if there are chain maps $f : F^\bullet \rightarrow G^\bullet$ and $g : G^\bullet \rightarrow F^\bullet$ such that $f \circ g$ is homotopic to id_{G^\bullet} and $g \circ f$ is homotopic to id_{F^\bullet} .

If f and g define a homotopy equivalence between F^\bullet and G^\bullet , then f and g are necessarily quasi-isomorphisms.

Definition 2.10. Let M be a d -parameter persistence module. A **presentation** of M is a homomorphism between free persistence modules $p : F^1 \rightarrow F^0$ such that $\text{Coker}(p) \cong M$. Write $q : F^0 \rightarrow \text{Coker}(p)$ for the canonical map; the presentation p is **minimal** if (1) q maps a basis of F^0 bijectively to a minimal homogenous set of generators of $\text{Coker}(p)$, and (2) p maps a basis of F^1 bijectively to a minimal homogenous set of generators of $\text{Ker}(q)$.

We give an example of a simplicial bi-filtration and a minimal presentation of its homology at the end of this section. Any presentation of a persistence module M can be obtained (up to isomorphism) from a minimal presentation p by taking the direct sum with maps of the form $\text{id}_H : H \rightarrow H$ or of the form $H \rightarrow 0$, where H is free. Following Lesnick-Wright [12], we say that a presentation is **semi-minimal** if it can be obtained from a minimal presentation by taking the direct sum with maps of the form $\text{id}_H : H \rightarrow H$, where H is free.

Graded matrices If F is a finitely-generated free d -parameter persistence module, and $B = \{B_i\}_{i \in I}$ is an ordered basis of F , then we can represent an element $v \in F_{\mathbf{z}}$ by a vector $[v]^B \in k^{|B|}$, as follows. If $\text{gr}(B_i) \not\leq \mathbf{z}$, we set $[v]_i^B = 0$.

Otherwise, we choose $[v]_i^B$ such that we have

$$v = \sum_{i: \text{gr}(B_i) \leq \mathbf{z}} [v]_i^B \cdot F_{\text{gr}(B_i), \mathbf{z}}(B_i).$$

Now, if $f : F \rightarrow F'$ is a homomorphism between finitely-generated free persistence modules, and B, B' are ordered bases of F, F' , we can represent f by a **graded matrix**, which is a matrix with entries in k such that each column and each row is annotated with a grade in \mathbb{Z}^d . In detail, f is represented by the graded matrix $[f]^{B, B'}$ whose j^{th} column is the vector $[f(B_j)]^{B'}$, and such that the grade of the j^{th} column is $\text{gr}(B_j)$, and the grade of the ℓ^{th} row is $\text{gr}(B'_\ell)$.

In this paper, the input to our algorithms will be chain complexes F^\bullet of finitely-generated free persistence modules, together with an ordered basis for each F^i . Therefore each homomorphism $\partial^n : F^n \rightarrow F^{n-1}$ is represented by a graded matrix. We assume that a graded matrix is stored in some sparse column representation, that is, the row indices of non-zero entries in a column, together with the entry in k , are stored in some container data structure. Moreover, we always assume that graded matrices have their rows and columns stored in an order that is compatible with the partial order on their grades, e.g., if the grade of column i is strictly less than the grade of column j , then $i < j$.

Definition 2.11. Let A be a graded matrix. If C is a non-zero column of A , the **pivot** of C is the largest row index j such that the j^{th} entry of C is non-zero. We call a non-zero column **local** if the grade of its pivot equals the grade of the column. In such a case, we call the pivot the **local pivot**.

We now present a small example of a minimal presentation that encodes the homology of a bi-filtration. We display the bi-filtration in Fig. 1. We work with \mathbb{Z}_2 coefficients.

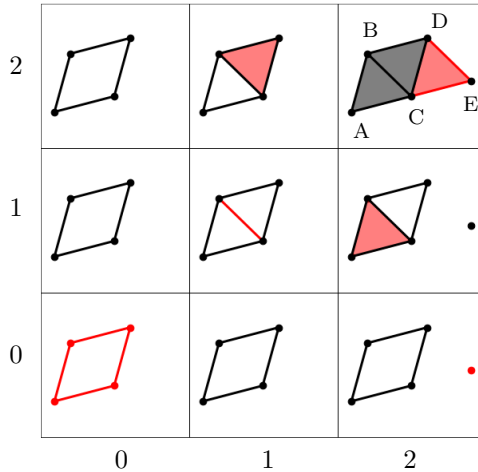


Figure 1: A simplicial bi-filtration. Simplices in red are at their minimal grade.

To compute the homology H^1 , we consider the boundary matrices:

$$[\partial^2] = \begin{array}{cc|ccc} & & ABC & BCD & DCE \\ & & (2,1) & (1,2) & (2,2) \\ \hline AB & (0,0) & 1 & 0 & 0 \\ AC & (0,0) & 1 & 0 & 0 \\ BC & (1,1) & 1 & 1 & 0 \\ BD & (0,0) & 0 & 1 & 0 \\ DC & (0,0) & 0 & 1 & 1 \\ CE & (2,2) & 0 & 0 & 1 \\ DE & (2,2) & 0 & 0 & 1 \end{array}$$

$$[\partial^1] = \begin{array}{cc|ccccccc} & & AB & AC & BC & BD & DC & CE & DE \\ & & (0,0) & (0,0) & (1,1) & (0,0) & (0,0) & (2,2) & (2,2) \\ \hline A & (0,0) & 1 & 1 & 0 & 0 & 0 & 0 & 0 \\ B & (0,0) & 1 & 0 & 1 & 1 & 0 & 0 & 0 \\ C & (0,0) & 0 & 1 & 1 & 0 & 1 & 1 & 0 \\ D & (0,0) & 0 & 0 & 0 & 1 & 1 & 0 & 1 \\ E & (2,0) & 0 & 0 & 0 & 0 & 0 & 1 & 1 \end{array}$$

The following graded matrix is a minimal presentation for the homology:

$$P = \begin{array}{cc|cc} & & (1,2) & (2,1) \\ \hline (0,0) & 1 & 0 \\ (1,1) & 1 & 1 \end{array}$$

Even in this toy example we see the compression achieved by passing to a minimal presentation. The minimal presentation encodes the homology up to isomorphism. In particular, from the minimal presentation we can read off the dimension of the homology of the bi-filtration at each grade. Write $P_{\leq \mathbf{z}}$ for the sub-matrix of P consisting of the columns and rows with grade less than or equal to \mathbf{z} ; then the homology at grade \mathbf{z} is isomorphic to the cokernel of $P_{\leq \mathbf{z}}$. For example, at $\mathbf{z} = (1,2)$, the homology has dimension equal to

$$\dim \text{coker } P_{\leq (1,2)} = \dim \text{coker } \begin{pmatrix} 1 \\ 1 \end{pmatrix} = 1.$$

Minimal presentations are not unique. In this case, the following graded matrix is also a minimal presentation:

$$P' = \begin{array}{cc|cc} & & (1,2) & (2,1) \\ \hline (0,0) & 0 & 1 \\ (1,1) & 1 & 1 \end{array}$$

As we will discuss in Section 4, computing a minimal presentation involves computing a basis for $\ker [\partial^1]$. The presentations P and P' correspond to different bases \mathcal{B} and \mathcal{B}' . Both \mathcal{B} and \mathcal{B}' include the cycle $AB + BD + DC + CA$ that is born at $(0,0)$, but \mathcal{B} has the cycle $AB + BC + CA$ at $(1,1)$, while \mathcal{B}' has the cycle $BC + CD + DB$ at $(1,1)$.

3 Multi-chunk compression

Given a chain complex F^\bullet of finitely-generated free persistence modules, together with an ordered basis for each F^n , we define a compression algorithm

called `multi-chunk` that returns a chain complex G^\bullet of finitely-generated free persistence modules such that:

- F^\bullet and G^\bullet are homotopy equivalent;
- given a chain complex \bar{F}^\bullet of finitely-generated free persistence modules quasi-isomorphic to F^\bullet , for any dimension n and any grade \mathbf{p} , the number of generators in G^n at \mathbf{p} is less than or equal to the number of generators in \bar{F}^n at \mathbf{p} .

3.1 Multi-chunk compression: Input and output settings

For the sake of clarity, `multi-chunk` is described for the case of 2-parameter persistence modules, and with $k = \mathbb{Z}_2$. The algorithm can easily be reformulated and generalized for an arbitrary base field and an arbitrary number of parameters.

Given a chain complex F^\bullet of finitely-generated free persistence modules and a dimension n , choose for each n a basis B^n of F^n . As in Section 2, for each basis B^n , we fix an ordering which is compatible with the grade. That is, for two generators g_1 and g_2 of B^n such that $\text{gr}(g_1) < \text{gr}(g_2)$, g_1 precedes g_2 .

As previously mentioned, the boundary homomorphism $\partial^n : F^n \rightarrow F^{n-1}$ is represented by a graded matrix $[\partial^n]^{B^n, B^{n-1}}$ whose columns are in correspondence with the generators of the basis B^n of F^n . Specifically, each column c (in correspondence with a generator g) encodes the boundary of g with respect to the basis B^{n-1} of F^{n-1} . Moreover, the columns and the rows of the matrix will be sorted in accordance with the ordering adopted by B^n and B^{n-1} . We will say that a generator g of B^n is of index i if it is in correspondence with the i^{th} column of the matrix $[\partial^n]^{B^n, B^{n-1}}$. Similarly, a generator g of B^{n-1} is of index i if it is in correspondence with the i^{th} row of the matrix $[\partial^n]^{B^n, B^{n-1}}$. Given two elements $c_1 \in F_{\mathbf{z}}^n$ and $c_2 \in F_{\mathbf{w}}^{n-1}$, we denote as $\langle c_1, c_2 \rangle$ the number (mod 2) of the generators of B^n appearing with a non-zero coefficient in the representations of c_1 and c_2 in terms of the elements of B^n .

In the following, we will assume that the data structure adopted for encoding the matrix $[\partial^n]^{B^n, B^{n-1}}$ will be able to store, for each column c , the following information:

- the index $i(c)$ of the corresponding generator g ;
- the grade of g ;
- the dimension of g ;
- the boundary of g (the list of the generators of B^{n-1} which appear with a non-zero coefficient in the boundary of g (as well as their indices, grades, and dimensions)).

By a small abuse of notation, in the following we will often write c in place of g and vice versa.

The algorithm `multi-chunk` takes as input the collection of graded matrices representing the boundary homomorphisms $\partial^n : F^n \rightarrow F^{n-1}$ and it returns a collection of graded matrices representing boundary homomorphisms $\partial^n : G^n \rightarrow G^{n-1}$.

Focusing on an example, the input of `multi-chunk` for the bi-filtration depicted in Figure 1 consists of the following boundary matrices:

$$[\partial^2]^{B^2, B^1} = \begin{array}{c|ccc} & & \begin{array}{c} ABC \\ (2, 1) \end{array} & \begin{array}{c} BCD \\ (1, 2) \end{array} & \begin{array}{c} CDE \\ (2, 2) \end{array} \\ \hline \begin{array}{c} AB \\ AC \\ BD \\ CD \\ BC \\ CE \\ DE \end{array} & \begin{array}{c} (0, 0) \\ (0, 0) \\ (0, 0) \\ (0, 0) \\ (1, 1) \\ (2, 2) \\ (2, 2) \end{array} & \begin{array}{c} 1 \\ 1 \\ 0 \\ 0 \\ 1 \\ 0 \\ 0 \end{array} & \begin{array}{c} 0 \\ 0 \\ 1 \\ 1 \\ 1 \\ 0 \\ 0 \end{array} & \begin{array}{c} 0 \\ 0 \\ 0 \\ 1 \\ 0 \\ 1 \\ 1 \end{array} \end{array}$$

$$[\partial^1]^{B^1, B^0} = \begin{array}{c|ccccccc} & \begin{array}{c} AB \\ (0, 0) \end{array} & \begin{array}{c} AC \\ (0, 0) \end{array} & \begin{array}{c} BD \\ (0, 0) \end{array} & \begin{array}{c} CD \\ (0, 0) \end{array} & \begin{array}{c} BC \\ (1, 1) \end{array} & \begin{array}{c} CE \\ (2, 2) \end{array} & \begin{array}{c} DE \\ (2, 2) \end{array} \\ \hline \begin{array}{c} A \\ B \\ C \\ D \\ E \end{array} & \begin{array}{c} (0, 0) \\ (0, 0) \\ (0, 0) \\ (0, 0) \\ (2, 0) \end{array} & \begin{array}{c} 1 \\ \mathbf{1} \\ 0 \\ 0 \\ 0 \end{array} & \begin{array}{c} 1 \\ 0 \\ \mathbf{1} \\ 0 \\ 0 \end{array} & \begin{array}{c} 0 \\ 1 \\ 0 \\ \mathbf{1} \\ 0 \end{array} & \begin{array}{c} 0 \\ 1 \\ 1 \\ 0 \\ 0 \end{array} & \begin{array}{c} 0 \\ 0 \\ 1 \\ 0 \\ 1 \end{array} & \begin{array}{c} 0 \\ 0 \\ 0 \\ 1 \\ 1 \end{array} \end{array}$$

expressed in terms of the following bases (already sorted with an ordering compatible with the grades): $B^0 = \{A, B, C, D, E\}$, $B^1 = \{AB, AC, BD, CD, BC, CE, DE\}$, and $B^2 = \{ABC, BCD, CDE\}$. In order to highlight them, the local pivots of the boundary matrices (which will play a crucial role in the first phase of `multi-chunk`) have been written in bold.

3.2 Multi-chunk compression: Algorithm

The algorithm `multi-chunk` works in three phases:

- *local reduction*;
- *compression*;
- *removal of local columns*.

The next paragraphs will be devoted to describing these phases. Pseudocode of the three phases is provided in B.

Phase I: Local reduction The goal of this phase is to perform a preliminary reduction of the graded matrices aimed at labelling the generators of each basis B^n as *global*, *local positive* or *local negative*.

We proceed in decreasing order with respect to the dimension n . The phase of local reduction works as follows on the graded boundary matrix $[\partial^n]^{B^n, B^{n-1}}$ (see Alg. 2). The algorithm traverses the columns in increasing order with respect to the index i and performs the following operations on a column c . If c (or better, its corresponding generator g) has been already labeled (as global,

local positive, or local negative), do nothing. Otherwise, as long as c has a local pivot (i.e., if the grade of the pivot of c equals the one of c) and there is a column c' with $i(c') < i(c)$ and the same local pivot as c , perform the column addition $c \leftarrow c + c'$. If at the end of this loop, the column c does not have a local pivot, label the column as global and proceed. Otherwise, label c as local negative and its local pivot c'' as local positive. In this case, (c'', c) is called a *local pair*.

Any column addition performed within the local reduction involves columns having the same grade. So, the local reduction operates independently on columns of different grade. We call blocks of columns with the same grade *chunks*; hence the name of the algorithm. As just discussed, operations on one chunk do not affect columns of any other chunk, hence the local reduction phase can be readily invoked in parallel on the chunks of the input matrix $[\partial^n]^{B^n, B^{n-1}}$.

A complete labeling of all the generators of the chosen bases of F^\bullet is achieved by applying local reduction to all the graded boundary matrices of F^\bullet . Finally, note that by proceeding in decreasing dimension, we avoid performing any column additions on local positive columns. This is reminiscent of the *clearing optimization* in the one-parameter version [16, 11].

Running Phase I of **multi-chunk** on the considered example, we obtain the following boundary matrices:

$$[\partial^2]^{B^2, B^1} = \begin{array}{c|ccc} & \begin{array}{c} ABC \\ (2,1) \end{array} & \begin{array}{c} BCD \\ (1,2) \end{array} & \begin{array}{c} CDE \\ (2,2) \end{array} \\ \hline \begin{array}{c} \textcolor{red}{AB} \\ \textcolor{red}{AC} \\ \textcolor{red}{BD} \\ CD \\ BC \\ CE \\ \textcolor{green}{DE} \end{array} & \begin{array}{c} (0,0) \\ (0,0) \\ (0,0) \\ (0,0) \\ (1,1) \\ (2,2) \\ (2,2) \end{array} & \begin{array}{c} \mathbf{1} \\ \mathbf{1} \\ 0 \\ 0 \\ 1 \\ 0 \\ 0 \end{array} & \begin{array}{c} 0 \\ 0 \\ \mathbf{1} \\ 1 \\ 1 \\ 0 \\ 1 \end{array} \end{array}$$

$$[\partial^1]^{B^1, B^0} = \begin{array}{c|ccccccc} & \begin{array}{c} \textcolor{red}{AB} \\ (0,0) \end{array} & \begin{array}{c} \textcolor{red}{AC} \\ (0,0) \end{array} & \begin{array}{c} \textcolor{red}{BD} \\ (0,0) \end{array} & \begin{array}{c} CD \\ (0,0) \end{array} & \begin{array}{c} BC \\ (1,1) \end{array} & \begin{array}{c} CE \\ (2,2) \end{array} & \begin{array}{c} \textcolor{green}{DE} \\ (2,2) \end{array} \\ \hline \begin{array}{c} A \\ \textcolor{green}{B} \\ \textcolor{green}{C} \\ \textcolor{green}{D} \\ E \end{array} & \begin{array}{c} (0,0) \\ (0,0) \\ (0,0) \\ (0,0) \\ (2,0) \end{array} & \begin{array}{c} 1 \\ 1 \\ 0 \\ 0 \\ 0 \end{array} & \begin{array}{c} 1 \\ 0 \\ 1 \\ 0 \\ 0 \end{array} & \begin{array}{c} 0 \\ 0 \\ 0 \\ 1 \\ 0 \end{array} & \begin{array}{c} 0 \\ \mathbf{1} \\ \mathbf{1} \\ 0 \\ 0 \end{array} & \begin{array}{c} 0 \\ 0 \\ \mathbf{1} \\ 0 \\ 1 \end{array} & \begin{array}{c} 0 \\ 0 \\ 0 \\ 1 \\ 1 \end{array} \end{array}$$

and the following local pairs: (DE, CDE) , (B, AB) , (C, AC) , (D, BD) . Columns and rows highlighted in red will correspond to local negative generators, while the green ones to local positive generators. The remaining columns and rows will correspond to global generators. Since they will play a crucial role in the Phase II of **multi-chunk**, local negative and local positive elements currently appearing in the boundary of global columns have been highlighted in bold.

Phase II: Compression The second phase of the algorithm aims at removing local (positive or negative) generators from the boundary of all global columns in the graded boundary matrices.

Given the modified graded boundary matrix $[\partial^n]^{B^n, B^{n-1}}$ returned by the previous step, the compression phase works as follows (see Alg. 3). For each

global column c , while the boundary of the column contains a generator that is local positive or local negative, the algorithm picks the local generator c' with maximal index.

- If c' is negative, remove c' from the boundary of c ;
- If c' is positive, denote c'' as the (unique) local negative n -column with c' as local pivot and perform the column addition $c \leftarrow c + c''$.

This ends the description of the compression phase. On termination, all the generators in the boundary of a global n -column are global.

The above process terminates for a column c because the index of the maximal local generator in the boundary of c is strictly decreasing in each step. That is clear for the case that c' is local negative. If c' is local positive, then c' is the generator in the boundary of c'' with the maximal index, so the column addition does not introduce in the boundary of c any generators with a larger index.

Note that the compression of a global column does not affect the result on any other global column. Thus, the phase can be parallelized as well.

Running Phase II of **multi-chunk** on the considered example, we obtain the following boundary matrices:

$$[\partial^2]^{B^2, B^1} = \begin{array}{c|ccc} & & \begin{array}{c} ABC \\ (2, 1) \end{array} & \begin{array}{c} BCD \\ (1, 2) \end{array} & \begin{array}{c} CDE \\ (2, 2) \end{array} \\ \hline \begin{array}{c} AB \\ AC \\ BD \\ CD \\ BC \\ CE \\ DE \end{array} & \begin{array}{c} (0, 0) \\ (0, 0) \\ (0, 0) \\ (0, 0) \\ (1, 1) \\ (2, 2) \\ (2, 2) \end{array} & \begin{array}{c} 0 \\ 0 \\ 0 \\ 0 \\ 1 \\ 0 \\ 0 \end{array} & \begin{array}{c} 0 \\ 0 \\ 0 \\ 1 \\ 1 \\ 0 \\ 0 \end{array} & \begin{array}{c} 0 \\ 0 \\ 0 \\ 1 \\ 0 \\ 1 \\ 1 \end{array} \end{array}$$

$$[\partial^1]^{B^1, B^0} = \begin{array}{c|ccccccc} & \begin{array}{c} AB \\ (0, 0) \end{array} & \begin{array}{c} AC \\ (0, 0) \end{array} & \begin{array}{c} BD \\ (0, 0) \end{array} & \begin{array}{c} CD \\ (0, 0) \end{array} & \begin{array}{c} BC \\ (1, 1) \end{array} & \begin{array}{c} CE \\ (2, 2) \end{array} & \begin{array}{c} DE \\ (2, 2) \end{array} \\ \hline \begin{array}{c} A \\ B \\ C \\ D \\ E \end{array} & \begin{array}{c} (0, 0) \\ (0, 0) \\ (0, 0) \\ (0, 0) \\ (2, 0) \end{array} & \begin{array}{c} 1 \\ 1 \\ 0 \\ 0 \\ 0 \end{array} & \begin{array}{c} 1 \\ 0 \\ 1 \\ 0 \\ 0 \end{array} & \begin{array}{c} 0 \\ 1 \\ 0 \\ 1 \\ 0 \end{array} & \begin{array}{c} 0 \\ 0 \\ 0 \\ 0 \\ 0 \end{array} & \begin{array}{c} 1 \\ 0 \\ 0 \\ 0 \\ 1 \end{array} & \begin{array}{c} 0 \\ 0 \\ 0 \\ 1 \\ 1 \end{array} \end{array}$$

Phase III: Removal of local pairs In the third phase of **multi-chunk**, we remove columns and rows from the boundary matrices.

Given the modified graded boundary matrices returned by the previous step, Phase III works as follows (see Alg. 4). Traverse all columns, and remove all columns labeled as local (positive or negative). Similarly, traverse all rows, and remove all rows labeled as local (positive or negative).

Let us denote by C^n the collection of generators of B^n in correspondence with the remaining (global) columns. The reduced matrices obtained by performing Phase III for all dimensions n can be considered as the graded boundary matrices $[\partial^n]^{C^n, C^{n-1}}$ representing the boundary homomorphisms $\partial^n : G^n \rightarrow G^{n-1}$ expressed in terms of the bases C^n and C^{n-1} .

Running Phase III of **multi-chunk** on the considered example, we obtain as output the following boundary matrices:

$$[\partial^2]^{C^2, C^1} = \begin{array}{c|cc} & ABC & BCD \\ & (2, 1) & (1, 2) \\ \hline CD & (0, 0) & 0 & 1 \\ BC & (1, 1) & 1 & 1 \\ CE & (2, 2) & 0 & 0 \end{array}$$

$$[\partial^1]^{C^1, C^0} = \begin{array}{c|ccc} & CD & BC & CE \\ & (0, 0) & (1, 1) & (2, 2) \\ \hline A & (0, 0) & 0 & 0 & 1 \\ E & (2, 0) & 0 & 0 & 1 \end{array}$$

expressed in terms of the following bases: $C^0 = \{A, E\}$, $C^1 = \{CD, BC, CE\}$, and $C^2 = \{ABC, BCD\}$.

3.3 Multi-chunk compression: Correctness

We prove that the output of **multi-chunk** is homotopy equivalent to the input. In order to do that,

- we introduce two elementary operations on chain complexes of finitely-generated free persistence modules;
- we prove that both elementary operations do not modify the homotopy type of the chain complex;
- we show that **multi-chunk** can be expressed by a sequence of such elementary operations.

Grade-preserving column addition Given distinct columns c, c' of a graded boundary matrix $[\partial^n]^{B^n, B^{n-1}}$, an operation of the form $c \leftarrow c + c'$ is called *grade-preserving* if $\text{gr}(c') \leq \text{gr}(c)$. Note that such an operation maintains the property that any generator c'' in the boundary of c satisfies $\text{gr}(c'') \leq \text{gr}(c)$, by transitivity of the grade.

Removal of local pair We call (c_1, c_2) a *local pair* if c_1 is a generator in B^n , c_2 is a generator in B^{n+1} , $\text{gr}(c_1) = \text{gr}(c_2)$ and c_1 is the local pivot of c_2 . We call *removal of the local pair* (c_1, c_2) the operation $\text{Del}(c_1, c_2)$ which acts on the graded boundary matrices of a chain complex F^\bullet as follows.

- For every $(n+1)$ -column c , replace its boundary $\partial^{n+1}(c)$ with $\partial^{n+1}(c) + \mu \partial^{n+1}(c_2)$, where μ is the coefficient of c_1 in $\partial^{n+1}(c)$. In particular, after this operation, c_1 disappeared from the boundary of any $(n+1)$ -columns. Moreover, notice that this operation is a grade-preserving column addition because the pair (c_1, c_2) is local, that is, $\text{gr}(c_1) = \text{gr}(c_2)$.
- For every $(n+2)$ -column c , update its boundary by setting the coefficient of c_2 in $\partial^{n+2}(c)$ to 0. In terms of matrices, this corresponds to removing the row corresponding to c_2 from $[\partial^n]^{B^{n+1}, B^n}$.
- Delete the generators c_1 and c_2 from B^n and B^{n+1} , respectively.

Grade-preserving column addition preserves homotopy type Given two n -columns c_1, c_2 such that $\text{gr}(c_1) \leq \text{gr}(c_2)$, the algorithm we propose allows for adding the boundary of column c_1 to the boundary of column c_2 . In this section, we formalize that in terms of modifications of chain complexes.

Given a chain complex $F^\bullet = (F^l, \partial^l)$ of finitely generated, free persistence modules, and distinct generators c_1, c_2 in the basis B^n with $\text{gr}(c_1) \leq \text{gr}(c_2)$, we define $\bar{F}^\bullet = (\bar{F}^l, \bar{\partial}^l)$ by setting:

- $\bar{F}^l = F^l$,
- for any $c \in B^l$,

$$\bar{\partial}^l(c) = \begin{cases} \partial^n(c) + \langle c, c_2 \rangle \partial^n(c_1) & \text{if } l = n, \\ \partial^{n+1}(c) + \langle \partial^{n+1}(c), c_2 \rangle c_1 & \text{if } l = n + 1, \\ \partial^l(c) & \text{otherwise.} \end{cases}$$

Let us define chain maps $f^\bullet : F^\bullet \rightarrow \bar{F}^\bullet$, $g^\bullet : \bar{F}^\bullet \rightarrow F^\bullet$ as follows:

- for any $c \in B^l$,

$$f^l(c) = \begin{cases} c + \langle c, c_2 \rangle c_1 & \text{if } l = n, \\ c & \text{otherwise;} \end{cases}$$

- for any $c \in B^l$,

$$g^l(c) = \begin{cases} c + \langle c, c_2 \rangle c_1 & \text{if } l = n, \\ c & \text{otherwise.} \end{cases}$$

Then, by a routine calculation we obtain the following:

Proposition 3.1. *The chain complexes of free persistence modules F^\bullet and \bar{F}^\bullet are isomorphic via the chain map f^\bullet and its inverse g^\bullet .*

Removal of local pair preserves homotopy type Given a local pair (c_1, c_2) of columns, the algorithm we propose allows for deleting them from the boundary matrix. In this section, we formalize that in terms of modifications of chain complexes.

Given a chain complex $F^\bullet = (F^l, \partial^l)$ of finitely generated, free persistence modules, and generators $c_1 \in B^n$ and $c_2 \in B^{n+1}$ such that $\langle \partial^{n+1}(c_2), c_1 \rangle \neq 0$ and $\text{gr}(c_1) = \text{gr}(c_2)$, we define $\bar{F}^\bullet = (\bar{F}^l, \bar{\partial}^l)$ by setting:

- \bar{F}^l as the free persistence module with basis

$$\bar{B}^l = \begin{cases} B^n - \{c_1\} & \text{if } l = n, \\ B^{n+1} - \{c_2\} & \text{if } l = n + 1, \\ B^l & \text{otherwise;} \end{cases}$$

- for any $c \in \bar{B}^l$,

$$\bar{\partial}^l(c) = \begin{cases} \partial^{n+1}(c) + \langle \partial^{n+1}(c), c_1 \rangle \partial^{n+1}(c_2) & \text{if } l = n+1, \\ \partial^{n+2}(c) + \langle \partial^{n+2}(c), c_2 \rangle c_2 & \text{if } l = n+2, \\ \partial^l(c) & \text{otherwise.} \end{cases}$$

Let us define chain maps $r^\bullet : F^\bullet \rightarrow \bar{F}^\bullet$, $s^\bullet : \bar{F}^\bullet \rightarrow F^\bullet$ as follows:

- for any $c \in B^l$,

$$r^l(c) = \begin{cases} c + \langle c, c_1 \rangle \partial^{n+1}(c_2) & \text{if } l = n, \\ c + \langle c, c_2 \rangle c_2 & \text{if } l = n+1, \\ c & \text{otherwise;} \end{cases}$$

- for any $c \in \bar{B}^l$,

$$s^l(c) = \begin{cases} c + \langle \partial^{n+1}(c), c_1 \rangle c_2 & \text{if } l = n+1, \\ c & \text{otherwise;} \end{cases}$$

Using these maps, we prove the following result (see A for a detailed proof):

Theorem 3.2. *The chain complexes of free persistence modules F and \bar{F} are homotopy equivalent.*

Multi-chunk algorithm preserves homotopy type By combining the previous results, we are now ready to prove the correctness of **multi-chunk**.

Theorem 3.3. *Let F^\bullet be a chain complex of finitely-generated free persistence modules together with an ordered basis for each F^n and let G^\bullet be the chain complex of finitely-generated free persistence modules returned by performing **multi-chunk** on F^\bullet . Then, F^\bullet and G^\bullet are homotopy equivalent.*

Proof. In order to prove the theorem we exhibit that **multi-chunk** can be expressed by a sequence of grade-preserving column additions and removals of local pairs. Because every column addition in Phase I is between columns of the same grade, all column additions are grade-preserving. Hence, after Phase I, the chain complex is equivalent to the input.

In Phase II, note that all column additions performed are grade-preserving. Indeed, if c' is in the boundary of column c , then $\text{gr}(c') \leq \text{gr}(c)$ holds. If c' is local positive, it triggers a column addition of the form $c \leftarrow c + c''$ with its local negative counterpart c'' . Since $\text{gr}(c') = \text{gr}(c'')$, $\text{gr}(c'') \leq \text{gr}(c)$ as well.

A further manipulation in Phase II is the removal of local negative columns from the boundary of global columns. These removals cannot be directly expressed in terms of the two elementary operations from above. Instead, we define a slight variation of our algorithm: in Phase II, when we encounter a local negative c' , we do nothing. In other words, the compression only removes

the local positive generators from the boundary c , and keeps local negative and global generators. In Phase III, instead of removing local columns, we perform a removal of a local pair (c_1, c_2) whenever we encounter a local negative column c_2 with local pivot c_1 . We call that algorithm **modified multi-chunk**. Note that this modified algorithm is a sequence of grade-preserving column additions, followed by a sequence of local pair removals, and thus produces a chain complex that is equivalent to the input F^\bullet .

We argue next that **multi-chunk** and **modified multi-chunk** yield the same output. Since both versions eventually remove all local columns, it suffices to show that they yield the same global columns. Fix an index of a global column, and let c denote the column of that index returned by the original chunk algorithm. Let c^* denote the column of the same index produced by the modified algorithm after the modified Phase II. The difference of c^* and c lies in the presence of local negative generators in the boundary of c^* which have been removed in c . The modified Phase III affects c^* in the following way: when a local pair (c_1, c_2) is removed, the local negative c_2 is, if it is present, removed from the boundary of c^* . There is no column addition during the modified Phase III involving c^* because all local positive columns have been eliminated. Hence, the effect of the modified Phase III on c^* is that all local negative columns are removed from its boundary which turns c^* to be equal to c at the end of the algorithm. Hence, the output of both algorithms is the same, proving the theorem. \square

3.4 Multi-chunk compression: Complexity

In order to properly express the time and the space complexity of the proposed algorithm, let us introduce the following parameters. Given input F^\bullet , we denote as n the number of generators of F^\bullet , as m the number of chunks, as ℓ the maximal size of a chunk, and as g the number of global columns. Moreover, we assume the maximal size of the support of the boundary of the generators of F^\bullet as a constant. The latter condition is always ensured for bi-filtered simplicial complexes of fixed dimension.

Theorem 3.4. *The algorithm **multi-chunk** has time complexity $O(m\ell^3 + g\ell n)$ and space complexity $O(n\ell + g^2)$.*

Proof. Due to the similarity between the two algorithms, the analysis of complexity of the proposed algorithm is analogous to the first two steps of the one-parameter chunk algorithm [11].

On the space complexity, during the Phase I, the generators in the boundary of any column can be at most $O(\ell)$. So, $O(n\ell)$ is a bound on the accumulated size of all columns after Phase I. During Phase II, the boundary of any global column can consist of up to n generators, but reduces to g generators at the end of the compression of the column because all local entries have been removed. Hence, the final chain complex has at most g entries in each of its g columns, and requires $O(g^2)$ space. Hence, the total space complexity is $O(n\ell + n + g^2)$,

where the second summand is redundant.¹ \square

We remark that the first term in the bound of Theorem 3.4 can actually be improved to $\min\{m\ell^3, n^3\}$ because in the worst case, the local reduction procedure (whose complexity is counted by this term) cannot perform more than $O(n^2)$ column operations, each of them costing at most $O(n)$ time.

3.5 Multi-chunk compression: Optimality

Let \bar{F}^\bullet be a chain complex of finitely generated free persistence modules. Let $\mathbf{p} = (p_x, p_y) \in \mathbb{Z}^2$, and define the vector space $\bar{F}_{<\mathbf{p}}^n$ to be the colimit of the restriction $\bar{F}^n|_{\mathbb{Z}_{<\mathbf{p}}^2} : \mathbb{Z}_{<\mathbf{p}}^2 \rightarrow \text{Vec}$, where $\mathbb{Z}_{<\mathbf{p}}^2 = \{\mathbf{z} \in \mathbb{Z}^2 : \mathbf{z} < \mathbf{p}\}$. Using the induced boundary homomorphisms, we obtain a chain complex $\bar{F}_{<\mathbf{p}}^\bullet$ of vector spaces. Equivalently, if we write $\mathbf{p}_0 = (p_x - 1, p_y - 1)$, $\mathbf{p}_1 = (p_x - 1, p_y)$, and $\mathbf{p}_2 = (p_x, p_y - 1)$, the vector space $\bar{F}_{<\mathbf{p}}^n$ can be defined by the short exact sequence:

$$0 \rightarrow \bar{F}_{\mathbf{p}_0}^n \rightarrow \bar{F}_{\mathbf{p}_1}^n \oplus \bar{F}_{\mathbf{p}_2}^n \rightarrow \bar{F}_{<\mathbf{p}}^n \rightarrow 0.$$

Moreover, let $\eta_{\mathbf{p}}^n$ be the homology map in dimension n induced by the inclusion of $\bar{F}_{<\mathbf{p}}^\bullet$ into \bar{F}^\bullet . We define

$$\delta_{\mathbf{p}}^n(\bar{F}^\bullet) := \dim \text{Ker } \eta_{\mathbf{p}}^{n-1} + \dim \text{Coker } \eta_{\mathbf{p}}^n,$$

and

$$\gamma_{\mathbf{p}}^n(\bar{F}^\bullet) := \dim \bar{F}_{\mathbf{p}}^n - \dim \bar{F}_{<\mathbf{p}}^n.$$

Theorem 3.5. *Let G^\bullet be the output of `multi-chunk` applied to the input F^\bullet . Then $\delta_{\mathbf{p}}^n(F^\bullet) = \gamma_{\mathbf{p}}^n(G^\bullet)$.*

The full proof is given in A and can be summarized as follows. Every global column with grade \mathbf{p} either destroys a homology class of $H(F_{<\mathbf{p}}^\bullet)$, or it creates a new homology class in $H(F_{\mathbf{p}}^\bullet)$, which is not destroyed by any other column of grade \mathbf{p} . Hence, each global column contributes a generator to $\text{Ker } \iota_{\mathbf{p}}^{n-1}$ or to $\text{Coker } \iota_{\mathbf{p}}^n$, where $\iota_{\mathbf{p}}^l$ is the map between the l^{th} homology spaces induced by the inclusion of $F_{<\mathbf{p}}^\bullet$ into $F_{\mathbf{p}}^\bullet$. Local columns do not contribute to either of these two spaces. The result follows from the fact that the number of global columns at grade \mathbf{p} is precisely the number of generators added at \mathbf{p} to G^\bullet .

The next statement shows that our construction is optimal in the sense that any chain complex of free persistence modules \bar{F}^\bullet that is quasi-isomorphic to F^\bullet must have at least as many generators as G^\bullet .

Theorem 3.6. *Any chain complex of free persistence modules \bar{F}^\bullet quasi-isomorphic to F^\bullet has to add at least $\delta_{\mathbf{p}}^n(F^\bullet)$ n -generators at grade \mathbf{p} . I.e., $\delta_{\mathbf{p}}^n(F^\bullet) \leq \gamma_{\mathbf{p}}^n(\bar{F}^\bullet)$.*

¹We remark that this bound only holds for the sequential version of the algorithm. In a parallelized version, it can happen that several compressed columns achieve a size of $O(n)$ at the same time.

The full proof is also given in A. To summarize, it is not too hard to see that, for any \bar{F}^\bullet quasi-isomorphic to F^\bullet , $\delta_{\mathbf{p}}^n(\bar{F}^\bullet) \leq \gamma_{\mathbf{p}}^n(\bar{F}^\bullet)$. Moreover, the quasi-isomorphism between F^\bullet and \bar{F}^\bullet implies that $\dim \text{Ker } \eta_{\mathbf{p}}^{n-1} = \dim \text{Ker } \iota_{\mathbf{p}}^{n-1}$ and $\dim \text{Coker } \eta_{\mathbf{p}}^n = \dim \text{Coker } \iota_{\mathbf{p}}^n$. So, $\delta_{\mathbf{p}}^n(F^\bullet) = \delta_{\mathbf{p}}^n(\bar{F}^\bullet)$, which implies that claim. The equality of the dimensions is formally verified using the Mayer-Vietoris sequence and the 5-lemma to establish an isomorphism from $H^n(F_{<\mathbf{p}}^\bullet)$ to $H^n(\bar{F}_{<\mathbf{p}}^\bullet)$ that commutes with the isomorphism at grade \mathbf{p} .

4 Mpfree compression

We now describe **mpfree**, our algorithm for computing minimal presentations of 2-parameter persistence modules. As with the description of **multi-chunk**, we fix the base field $k = \mathbb{Z}_2$ for simplicity, but the algorithm can easily be reformulated for an arbitrary base field. We assume the number of parameters d is 2. For **mpfree** this assumption is not simply for convenience. For $d > 2$, the methods of this section do not immediately apply.

4.1 Mpfree compression: Input and output settings

In Section 3 we assume that bases of free persistence modules are ordered in a way that is compatible with the partial order on the grades of the basis elements. We now strengthen this assumption, and assume that bases of free persistence modules are in co-lexicographic order with respect to grades, with basis elements of the same grade ordered arbitrarily. In particular, the graded matrices in this section have columns and rows that are in co-lexicographic order with respect to grades. We explain the significance of this assumption when we describe the column operations performed by the algorithm.

As explained in the introduction, **mpfree** is a modified version of an algorithm of Lesnick and Wright, which we call the LW algorithm. The LW algorithm takes as input a short chain complex

$$F^2 \xrightarrow{\partial^2} F^1 \xrightarrow{\partial^1} F^0$$

of finitely generated free 2-parameter persistence modules, and returns a minimal presentation of the homology of this chain complex. More precisely, the input consists of graded matrices A and B , representing ∂^2 and ∂^1 respectively.

The LW algorithm consists of four steps, where the first three compute a semi-minimal presentation M' , and the fourth step computes a minimal presentation M from M' ; our algorithm **mpfree** shares this structure.

Min_gens Computes a minimal ordered set of generators G of the image of A .

Ker_basis Computes an ordered basis K of the kernel of B .

Reparam Re-expresses every element of G as a linear combination in K , keeping its grade. This is possible since $BA = 0$. The resulting graded matrix M' is a semi-minimal presentation.

Minimize Identifies pairs (g, r) of generators (rows in M') and relations (columns in M') where r “eliminates” g and both r and g have the same grade. In that case, row g and column r are removed from M' after some algebraic manipulations without changing the persistence module. Removing all such pairs results in a minimal presentation M .

The difference between the LW algorithm and **mpfree** is in how these steps are implemented. We will now describe the LW algorithm, and then describe our improvements. We give pseudocode in B.

4.2 Mpfree compression: The Lesnick–Wright algorithm

As we assume $d = 2$, each column and row of the graded matrices A and B come with a grade in \mathbb{Z}^2 . We assume that every x -coordinate of a grade of a column of A or B is in $\{1, \dots, X\}$ and every y -coordinate in $\{1, \dots, Y\}$. Hence, we can visualize A and B via a $X \times Y$ integer grid, where each grid cell contains a (possibly empty) sequence of matrix columns. Traversing the grid row by row upwards yields the co-lexicographic order of the matrix. We will phrase the algorithms for **Min_gens** and **Ker_basis** with this interpretation. To illustrate the algorithm we show how each step acts on our running example, displayed in Fig. 1.

Details of Min_gens The procedure traverses the columns of A in a certain order defined below. During the traversal, it maintains a **pivot map** ρ , a partial map from row indices to column indices. The interpretation is that $\rho(i) = j$ if column j has been visited, has pivot i , and there is no visited column j' with pivot i and $j' < j$. Initially, ρ is the empty map, reflecting the state that no column has been visited.

At any point of the algorithm, **reducing** a column j means the following operation (Alg. 5): as long as j is not empty, has pivot i and $\rho(i) = j'$ with $j' < j$, add column j' to column j . This results in cancellation of the pivot (since the coefficients are in \mathbb{Z}_2) and hence, after the addition, the pivot of j is strictly smaller than i (or the column is empty). In either case, the reduction terminates after finitely many iterations, and column j is marked as visited. If it ends with a non-empty column with pivot i , set $\rho(i) \leftarrow j$.

We can now describe the procedure **Min_gens** (see Alg. 6): Using the grid interpretation from above, traverse the grid cells in lexicographic order; that means, the grid is traversed column by column from the left, traversing each column bottom-up. When reaching grid cell (x, y) , iterate through all matrix columns with grade $(1, y), (2, y), \dots, (x-1, y)$ in that order (i.e., through all cells on the left of (x, y)) and reduce them as described above. Then, iterate through the matrix columns at grade (x, y) and reduce them as well. Append every column at grade (x, y) not reducing to 0 in the output matrix, with grade (x, y) .

The combination of the co-lexicographic order of the columns and the lexicographic order in which we traverse the grid has the following effect. If we add

column j' to column j , then $j' < j$ and thus $\text{gr}(j') \leq \text{gr}(j)$ in co-lexicographic order; furthermore, j' must be in the image of the pivot map, and thus j' has been visited and therefore $\text{gr}(j') \leq \text{gr}(j)$ in lexicographic order. It follows that $\text{gr}(j') \leq \text{gr}(j)$ in the usual partial order on \mathbb{Z}^2 , which is crucial for the correctness of the algorithm.

Assuming $y \neq 1$, when we finish handling all columns at grade $(x, y-1)$, the sub-matrix of A consisting of columns with grade less than or equal to $(x, y-1)$ (in the usual partial order on \mathbb{Z}^2) is reduced. Therefore, when we consider the grade (x, y) , in order to reduce the sub-matrix consisting of columns with grade less than or equal to (x, y) , we only need to reduce the columns with grade $(1, y), \dots, (x, y)$. See [12] for more details.

The sub-routine **Min_gens** has no work to do on our running example, but **Ker_basis** will have work to do, and the action of this sub-routine will illustrate the matrix reduction involved also in **Min_gens**.

Details of Ker_basis This procedure is similar to the previous one, as it visits the columns in the same order, and reduces them when visiting. There is one difference in the reduction procedure, however: every column maintains an **auxiliary vector**. Initially, the auxiliary vector of column j is just the unit vector e_j and whenever column j' is added to column j , we also add the auxiliary vector of j' to the auxiliary vector of j . In linear algebra terms, the auxiliary vectors yield an auxiliary matrix S (which is the identity matrix initially) and letting B' denote the matrix arising from B at any point of the algorithm, we maintain the invariant that $B' = BS$. In particular, if the j -th column of B' is 0, the j -th column of S encodes the linear combination of the columns of B that represents a kernel element of the linear map B .

We describe the procedure **Ker_basis** (Alg. 7): Traverse the grid cells in lexicographic order. When reaching grid cell (x, y) , iterate through all matrix columns with grade $(1, y), (2, y), \dots, (x, y)$ (in that order) and reduce them as described above. If any of these columns turn from non-zero to zero during the reduction, append the auxiliary vector of the column to the output matrix and set the grade of this column to (x, y) . The resulting matrix encodes the kernel basis of B . Its rows correspond to the columns of B and thus inherit their grades, yielding a graded matrix as output.

In order to apply **Ker_basis** to the matrix $[\partial^1]$ of our running example (displayed in Section 2), we need to put the columns in co-lexicographic order. We fix the order $AB, AC, BD, DC, BC, CE, DE$. After the matrix reduction, the columns corresponding to DC, BC , and DE are reduced to zero, and the output of **Ker_basis** is:

	(0,0)	(1,1)	(2,2)
(0,0)	1	1	1
(0,0)	1	1	1
(0,0)	1	0	1
(0,0)	1	0	0
(1,1)	0	1	0
(2,2)	0	0	1
(2,2)	0	0	1

This gives us the basis $\{AB + BD + DC + CA, AB + AC + BC, AB + AC + BD + CE + DE\}$ for the kernel of $[\partial^1]$.

Details of Reparam Let G denote the result of `Min_gens` and K the result of `Ker_basis`. Note that G and K have the same number of rows, with consistent grades. Form the matrix $(K|G)$ and reduce each column of G , using auxiliary vectors. It is guaranteed that this turns the matrix into $(K|0)$, and the auxiliary vectors of the columns of G yields a graded matrix M' which is the output of the procedure (Alg. 8).

Returning to our running example, the image of $[\partial^2]$ is generated by $G = \{\partial^2(ABC), \partial^2(BDC), \partial^2(DCE)\}$. Re-expressing these with respect to our basis for the kernel of $[\partial^1]$, we obtain the following semi-minimal presentation:

$$M' = \begin{array}{c|ccc} & (2,1) & (1,2) & (2,2) \\ \hline (0,0) & 0 & 1 & 1 \\ (1,1) & 1 & 1 & 0 \\ (2,2) & 0 & 0 & 1 \end{array}$$

Details of Minimize Let n denote the number of columns of M' , the output of the previous step. Traverse the columns of M' from index 1 to n . If column i is a local column (i.e., the grade of its pivot coincides with the column grade), let j denote its pivot and iterate through the columns $i + 1$ to n ; if any column k contains row index j , add column i to column k (eliminating the row index at j). At the end of this inner loop, no column except i has a non-zero entry at index j . We can therefore remove column i and row j from the matrix, without changing the persistence module that M' presents. So, remove column i and row j from the matrix. After the outer loop has finished, re-index the remaining rows and columns, and return the resulting graded matrix M as the minimal presentation (Alg. 9). Note that the inner loop of `Minimize` can be parallelized.

Applying `Minimize` to the semi-minimal presentation M' of our running example, we remove the single local column and obtain the following minimal presentation:

$$\begin{array}{c|cc} & (2,1) & (1,2) \\ \hline (0,0) & 0 & 1 \\ (1,1) & 1 & 1 \end{array}$$

4.3 Mpfree compression: Improvement via queues

We now describe methods to improve the performance of `Min_gens` and `Ker_basis`. We describe an improvement to `Minimize` in Section 4.4. In Section 5 we demonstrate the improvement in performance on several classes of input data.

In the worst case, the size of the grid used in `Min_gens` and `Ker_basis` is quadratic in the size of the input. It can happen, therefore, that simply storing and iterating over the grid can lead to quadratic behavior of the LW algorithm (see e.g. the “Points on sphere” data in Section 5).

One way around this is to control the size of the grid by coarsening: we choose a coarser grid in \mathbb{Z}^2 and snap each grade appearing in the matrices A and B to the closest grade in the coarser grid. Of course, this comes at the cost

of computing an approximate solution to the original problem. See Table 1 in Section 5 for the effect of this coarsening on the LW algorithm. We now show that coarsening is not necessary, as `Min_gens` and `Ker_basis` can be adapted so that their performance is indifferent to the size of the grid.

First note that it is not sufficient to only consider the grades of the matrix columns in `Min_gens` and `Ker_basis`. For instance, columns of B on grades (x', y) and (x, y') with $x' < x$ and $y' < y$ might combine into a kernel element at grade (x, y) , so `Ker_basis` has to perform work at grade (x, y) even if no column exists at this grade.

The main observation is that we can predict the grades on which the algorithm has to (potentially) perform operations, effectively avoiding the iteration through all grid cells. Surely, every grade that appears as a grade of matrix columns must be considered, to visit these columns for the first time. Moreover, consider the situation that the algorithm is at grade (x, y) and reduces a column with index i . Assume further that the pivot j of i appears already in ρ for an index $k > i$. In that case, the LW-algorithm updates $\rho(j) \leftarrow i$ and stops the reduction. However, we know more: the next time that column k is visited, column i , or perhaps some other column with pivot j , will be added to k . When is this next time? Since $i < k$ and the columns are in colex order, we know that y , the y -grade of i , is smaller than or equal to y' , the y -grade of k . If $y' = y$, column k will be handled in the same iteration, and nothing needs to be done. If $y' > y$, we know that the algorithm needs to consider grade (x, y') .

Based on this idea, we set up a priority queue that stores the grid cells that need to be visited, in lexicographic order. The queue is initialized with the column grades of the matrix. Then, instead of iterating over all grid cells, the algorithms `Min_gens` and `Ker_basis` keep popping the smallest element from the queue until the queue is empty, and proceed on each grade as described before. We extend the reduction method of a column as follows (Alg. 10): Whenever the algorithm encounters a situation as above during a column reduction, it pushes (x, y') to the queue. Every element pushed to the queue is necessarily lexicographically larger than the current element, so the algorithm terminates – in the worst case after having handled every grid cell once, but skipping over many grid cells in practice.

Proposition 4.1. *Using a priority queue for the grades as described, the algorithms `Min_gens` and `Ker_basis` produce the same output as in the LW algorithm.*

Proof. The argument is mostly the same for `Min_gens` and `Ker_basis`, and we just talk about “the algorithm” for either of them. More precisely, we refer to the LW version of the algorithm and the optimized version of the algorithm when talking about the variant without and with the priority queue, respectively.

We call a grade (x, y) *significant* if the algorithm, on grade (x, y) performs a column operation on the matrix or appends a column to the output matrix. We show that every significant grade in the LW algorithm is added to the priority queue in the optimized version. That proves that the outcome is the same using an inductive argument.

Fix a grade (x, y) and assume that the algorithm (in the LW version) performs a column operation in this iteration. Let i be the smallest index on which such an operation is performed, let j be its pivot, and let (x', y) be its grade with $x' \leq x$. If $x' = x$, then there is a matrix column with grade (x, y) and the grade is pushed into the grade priority queue initially. Otherwise, if $x' < x$, column i has been reduced previously in grade $(x - 1, y)$, and the reduction ended with $\rho(j) = i$ (otherwise, a further column addition would have been performed). The fact that a column addition is needed at grade (i, j) means that $\rho(j)$ must have been re-set, to an index smaller than i . However, between $(x - 1, y)$ and (x, y) , the algorithms iterated over the grades $(x - 1, y + 1), (x - 1, y + 2), \dots, (x - 1, Y), (x, 1), (x, 2), \dots, (x, y - 1)$ with Y the maximal y -grade. Note that in the first part of the sequence, with x -grade $x - 1$, only columns with index $> i$ are updated because the matrix is stored in colex order. Hence, none of these iterations can set $\rho(j)$ to a smaller index. It follows that the update of $\rho(j)$ happens at a grade with x -grade x . But then, the updated reduction algorithm ensures when $\rho(j)$ is updated, the grade (x, y) is added to the priority queue in this step.

Finally we consider the case that at grade (x, y) , the algorithm appends an output element. If the algorithm is **Min_gens**, this only happens when the grade appears as matrix column, and as argued earlier, these grades are added to the priority queue. For **Ker_basis**, an output column is added if a column is reduced from non-zero to zero, and this implies that at least one column addition was performed, so the grade is considered by the first part. \square

A further improvement is based on a very similar idea: note that when a grade (x, y) is handled, both **Min_gens** and **Ker_basis** still scan through all columns of grade (x', y) with $x' \leq x$ and reduce all columns in this range. Since only a few columns in this range typically need an update, most of the time in the algorithm is wasted scanning through this range.

Necessary updates can be predicted during earlier steps in the algorithm: as above, when, at grade (x, y) column i is reduced and its pivot is found in a column $k > i$, we know that column k needs an update. Let $y' \geq y$ be the y -grade of k . We can just remember the index k and handle it the next time when y -grade y' is visited, which will be at grade (x, y') .

Technically, we realize this idea by storing one priority queue per y -grade. In the extended column reduction, in a situation as above, the index k is pushed to the priority queue of its y -grade. When handling a grade (x, y) , instead of scanning through the columns of grade $(1, y), \dots, (x - 1, y)$, we keep popping the smallest index from the priority queue of y and reduce the column (this might introduce new elements to the priority queue, if $y = y'$ with the notation from above, but new elements are of larger index, so the procedure eventually empties the queue). After the queue is empty, the algorithm proceeds with the columns on grade (x, y) as in the LW-version. See Alg. 11 and 12 for pseudocode.

Proposition 4.2. *Using one priority queue per y -grade as described, the algorithms **Min_gens** and **Ker_basis** produce the same output as in the LW algorithm.*

Proof. Again, we argue inductively that the same column operations are performed in the variant without and with priority queues. Fix a column i for which the LW variant (without priority queues) performs a column operation for grade (x, y) . It suffices to show that i is pushed to the priority queue for y . If i is at grade (x, y) , it is pushed by the algorithm as specified, so we can assume that its grade is (x', y) with $x' < x$.

Let j be the pivot of column i . As in the previous proof, the fact that a column addition is performed means that $\rho(j)$ has been updated during the algorithm since i was visited at grade $(x - 1, y)$, and this can only happen at a grade (x, y') with $y' \leq y$. By the modified reduction method, i will be pushed into the priority queue of y in this case. \square

4.4 Mpfree compression: Improvement to minimization

We now explain how the performance of **Minimize** can be improved. The modification is similar in spirit to the queue optimizations: we improve the runtime by avoiding unnecessary scanning for columns that need to be updated.

Recall that, whenever **Minimize** identifies a local pair, the algorithm scans to the right to eliminate the local row index. Simply performing this scan can lead to quadratic time complexity. Typically, the row index only appears in a few columns, and the scan will query many columns that are not updated. Additionally, looking for a fixed row index is a non-constant operation for most representations of column data. For instance, if the column is realized as a dynamic array, it requires a binary search per column.

We can avoid both scanning and binary search by not eliminating local row indices immediately when they are identified as local. Instead, we simply apply **multi-chunk** to the short chain complex $F^1 \xrightarrow{M'} F^0 \rightarrow 0$, where M' is the semi-minimal presentation produced by **Reparam**.

Proposition 4.3. *If P is a semi-minimal presentation of a persistence module W , and Q is the graded matrix obtained from P by applying **multi-chunk**, then Q is a minimal presentation of W .*

Proof. Since the LW minimization algorithm produces a minimal presentation from P , it suffices to show that **multi-chunk** removes the same number of row-column pairs at each grade as the LW minimization algorithm. So, let \mathbf{z} be a grade of a column of P , and let $P_{\mathbf{z}}$ be the sub-matrix of P consisting of the columns and rows of P with grade \mathbf{z} . To complete the proof, we show that the number of row-column pairs with grade \mathbf{z} removed by the LW minimization algorithm and the number of row-column pairs with grade \mathbf{z} removed by **multi-chunk** are both equal to the rank of the matrix $P_{\mathbf{z}}$. Say that a matrix N has the “distinct pivot” property if any pair of non-zero columns of N have distinct pivots. Note that if N has the distinct pivot property, then the rank of N is the number of non-zero columns of N . The column operations performed by the LW minimization algorithm do not change the rank of $P_{\mathbf{z}}$, and after performing all column operations, the sub-matrix $P_{\mathbf{z}}$ has the distinct pivot

property, and the columns with grade \mathbf{z} removed by the LW minimization algorithm are the non-zero columns of this matrix. Similarly, the column operations performed by `multi-chunk` do not change the rank of $P_{\mathbf{z}}$, and after performing all column operations, the sub-matrix $P_{\mathbf{z}}$ has the distinct pivot property, and the columns with grade \mathbf{z} removed by `multi-chunk` are the non-zero columns of this matrix. \square

4.5 Mpfree compression: Complexity

It is easy to see that `mpfree` has the same worst-case behavior as the LW algorithm:

Theorem 4.4. *Let A be a $(b \times c)$ -matrix and B be an $(a \times b)$ -matrix. Then, `mpfree` runs in*

$$O((a + b + c)^3)$$

time and

$$O(b(a + b + c))$$

space in the worst case.

Proof. The first three steps of `mpfree` perform exactly the same matrix operations as the corresponding steps of the LW algorithm, and the complexity bound (in terms of time and memory) is dominated by these matrices and column operations on them. Hence, the same analysis as in [12, Sec 4.1] applies and yields the desired bound for the first three steps. The additional costs of maintaining priority queues is negligible, because the maximal number of operations on these queues is $O((a + b + c)^2)$, and each operation only needs logarithmic time. Moreover, the total number of elements in all queues is $O(bc)$ for `Min_gens` and $O(ab)$ for `Ker_basis`, so also the memory bound is satisfied.

For the minimization procedure, note that the semi-minimal presentation is a $(b \times c)$ -matrix, and we apply `multi-chunk` on it. In the notation of the complexity analysis of Section 3, $n \leftarrow b + c$, and g and ℓ are both bounded by n . By Theorem 3.4 and the subsequent remark, we get a worst-case complexity of $O(n^3)$ and space complexity of $O(n^2)$ which proves the theorem. \square

To make our improvements “visible” in a complexity analysis, we have to express the complexity of the algorithm using different parameters. We focus on the time complexity. Let M' denote the total number of column additions during the algorithm, and M denote the total cost to perform them. Note that M' is quadratic in the input size in the worst case, and $M = O(nM')$ which has led to our cubic bound in the previous theorem. However, in practice, we can expect that M and M' are much smaller than what the worst case predicts, similar to the one-parameter case. Revisiting the LW algorithm, we can express the complexity of `Min_gens` and `Ker_basis` as $O(M + XY)$, where X and Y are the grid dimensions of the instance. This is because the subroutines iterate over all cells of the grid. In particular, the $O(XY)$ factor appears in practice in every instance, which is visible for input with a large grid size.

In contrast, `mpfree` rather has a complexity of $O(M + M' \log n)$ because in the worst case, there is one priority queue operation triggered by every column operation. Note that if M and M' are linear in n (which is to be expected for realistic inputs), the algorithm shows a complexity of $O(n \log n)$, independently of the grid size.

For the minimization procedure, we still denote by M the total cost of all column additions. Then, the LW algorithm runs its minimization in $O(M + n^2 \log n)$ time, where the second term is due to the scanning to the right, looking for a row index to be cleared. Note again that this scan is performed every time a row index is removed so we have to expect a quadratic time behavior on every instance. In contrast, `mpfree` uses `multi-chunk` to avoid the scan. We can bound its complexity by $O(M + \Delta)$, where Δ is the cost of the compression step apart from the column additions performed.² Δ is proportional to the number of non-zero entries encountered in the presentation matrix, which can be quadratic in the worst case if the matrix becomes dense. However, this is not to be expected in most cases, and assuming that the matrix remains sparse and M is linear as before, the minimization step shows linear behavior.

5 Experimental results

We implemented both described algorithms in C++ and provide them as software repositories [13, 14] under the LGPL license.

Software design A few notable aspects of our code:

Both algorithms accept inputs in the `scc2020` format [39] and write their result in the same format. `multi-chunk` reads a chain complex of arbitrary length k and outputs a chain complex of same length, potentially with fewer generators. `mpfree` reads a chain complex of length 2 and outputs a chain complex of length 1, encoding the minimal presentation.

Both algorithms come as a sequential version and a shared-memory parallelized version using the `OpenMP` library. This is achieved just by adding the line

```
#pragma omp parallel for schedule(guided,1)
```

in front of the loops to be run in parallel (see the documentation of `OpenMP` for the details of the command). We have parallelized the compression procedure of `multi-chunk`, the reparameterization and the minimization procedure of `mpfree`, and some parts of the input processing. Unless stated otherwise, we will use the parallelized version throughout our experiments.

Our algorithms are *generic* in the sense that they operate on any graded matrix with a well-defined interface using the template mechanism of C++.

²We remark that the M in this step is not exactly equal to the M in the LW algorithm because the columns additions are not identical. Experimentally, we observed that the two costs are of similar size.

This allows our code, in particular, to run on every matrix representation that is provided by the PHAT library. In [18], we compared all choices and found out that the `vector_vector` representation was generally a good choice, so we use that representation throughout our experiments.

Experimental setup Our code was compiled with gcc-7.5.0, and ran on a workstation with an Intel(R) Xeon(R) CPU E5-1650 v3 CPU (6 cores, 12 threads, 3.5GHz) and 64 GB RAM, running GNU/Linux (Ubuntu 16.04.5). We measured the overall time and memory consumption using the linux command `/usr/bin/time`, and the `timer` library of the BOOST library to measure the time for subroutines.

We used the versions of `multi-chunk`, `mpfree`, and RIVET available in their bitbucket/github repositories on 6 July 2022.

The scripts for generating the input data and running the experiments, as well as the input files, are available [40]. This repository also contains the output files of the experiments, which contain the data on time and memory consumption that is summarized in the tables in this section.

To test the performance, we consider six different classes of input data of different sizes, resulting in a total of around 50 GB of data (uncompressed). In each case the number of parameters d is 2. With one exception, these data sets are artificial; our goal was to model input types that appear in practice and to still have some control over the input sizes. For each combination of class and parameters, we generated 5 instances and display the average in the tables. Our classes are in detail:

Full function Rips We sample n points from a noisy circle and consider the simplicial complex consisting of all n points, $e = \binom{n}{2}$ edges and $f = \binom{n}{3}$ triangles. The first coordinate of the bi-grade is 0 for vertices, the distance between endpoints for edges, and the length of the longest edge for triangles. This is the *Vietoris-Rips filtration*, one of the most prominent filtrations in topological data analysis. For the second grade coordinate, we used (the negative of) a kernel density estimate with Gaussian kernel with fixed bandwidth for the vertices, and this is extended to edges and triangles by assigning the maximal grade among the boundary vertices. We take the negative of the density estimate so that points in high-density regions appear at smaller grades than points in low-density regions. The construction ensures that the subcomplex at each grade is a *flag complex*, that is, a complex that is completely determined by its vertices and edges. This yields a chain complex of length 2 with generators f, e, n . Note that the number of generators is very imbalanced in this example, and the large number of triangles restricts the number of vertices (our largest instance has 289 points).

Function Rips with threshold We sample n points on a sphere in \mathbb{R}^3 (with non-uniform density) and fix a target number N of simplices. We then

build the Vietoris-Rips filtration on these vertices up to 3-simplices, until it consists of N simplices. The second coordinate of the bi-grade is determined as in the previous case, except that a linear kernel was used for efficiency. We choose N as large as 16 million, and always choose n to be $0.05 \cdot N$, so that 5% of the simplices are vertices. This leads to chain complexes of length 3 with many more generators at level 0 (up to 800,000) and a more balanced distribution of generators across the levels.

Points on sphere We generate the convex hull of n points on a sphere in \mathbb{R}^3 sampled uniformly at random. By Euler’s formula, the convex hull consists of exactly $e = 3n - 6$ edges and $f = 2n - 4$ triangles. The grades of a vertex are simply its x - and y -coordinates (ignoring the z -coordinate), and the x -/ y -grades of an edge and a triangle is just the maximal x -/ y -coordinate among its boundary vertices. This is also known as the *lower star (bi-)filtration* which generalizes a commonly used filtration type for a single parameter and has been used as a benchmark example in previous multi-parameter work [35]. Our largest instances consist of 1.6 million vertices.

Random Delaunay triangulations As a variant of the previous example, we sample n points inside the unit sphere, and we compute the Delaunay triangulation of these n points (using CGAL [41]). As before, we assign to vertices their x - and y -coordinates as grades, and to edges, triangles, and tetrahedra using the maximal grade of the boundary vertices. This results in a chain complex of length 3 with rather balanced numbers of generators. Our largest instances consists of 640,000 vertices.

Multi-cover bi-filtration We generated bi-filtrations coming from multi-covers of point clouds: the simplicial complex at grade (r, k) represents the region of the plane covered by at least k balls of radius r around the input points. A recent result [42] shows how to compute this structure efficiently based on rhomboid tiling [43]. In our examples, the maximal k is set to 10. Running the LW algorithm, this leads to a grid with only 10 different grades in the y -direction. Also, when picking points in \mathbb{R}^3 , the rhomboid tiling is 4-dimensional, resulting in a chain complex of length 4. Our largest instances pick 390 points in \mathbb{R}^3 , resulting in chain complexes with around 16 million generators.

Off-datasets We also tested with triangular mesh data, publicly available at the AIM@SHAPE repository³. The graded input matrices (A, B) were generated in the same way as for the previously described sphere and random Delaunay meshes. In this experiments, we restrict to the four datasets “hand”, “eros”, “dragon” and “raptor”, each yielding a chain complex of length 2 with 0.16, 2.4, 3.2 and 5.0 million simplices, respectively.

³available at <http://visionair.ge.imati.cnr.it/>

Comparison with RIVET We demonstrate that our improvements over the original algorithm by Lesnick and Wright [12] are highly effective. For that, we present a comparison of **mpfree** with the minimal presentation algorithm of RIVET. By comparing the numbers for **mpfree** and RIVET in Table 1, we see a clear improvement in time and memory.

We remark that both the usage of priority queues and of using **multi-chunk** for the minimization procedure lead to substantial speed-ups. This was demonstrated carefully in the conference version [18]. We cannot re-do these experiments because **mpfree** has no option to switch off these optimizations.

The main purpose of RIVET is the visualization of a 2-parameter module; for that reason, the input grades are usually snapped to an $x \times y$ -grid before further processing. While the implementation of the LW-algorithm in RIVET does not require snapping, it has not been optimized for large grids. Therefore, we ran the two algorithms on the same instances after snapping all bi-grades to a (uniformly chosen) 50×50 grid. As expected, RIVET becomes significantly faster and more memory efficient. However, **mpfree** is still faster even without snapping the input. In fact, **mpfree**’s performance after snapping improves by a factor of less than 2 in terms of time and memory for all inputs, so we do not include it in Table 1.

Class	N	Original				Snapped	
		RIVET		mpfree		RIVET	
		Time	Memory	Time	Memory	Time	Memory
FFR	253K	13.8	98MB	0.58	74MB	11.5	97MB
	508K	30.4	205MB	1.29	148MB	25.9	223MB
	1.02M	71.5	455MB	3.14	302MB	58.9	503MB
PoS	37K	16.9	3.11GB	0.12	31MB	1.92	24MB
	75K	68.0	12.4GB	0.25	64MB	5.32	48MB
	150K	381	49.3GB	0.57	138MB	16.9	103MB
MCF	40K	1.81	25MB	0.11	25MB	1.75	24MB
	100K	9.40	79MB	0.29	69MB	8.18	81MB
	199K	34.7	205MB	0.61	156MB	28.6	212MB
OFF	172K	>3600	35.3GB	0.77	145MB	8.59	193MB

Table 1: Time and memory comparison with the RIVET library. From left to right: class of input, number of generators, running time (in seconds) and memory consumption (three times).

Performance of multi-chunk See Table 2 for the performance of **multi-chunk** (parallel version). Note that the instances are much larger than for the RIVET comparison from Table 1. Generally, we can say that the running time of **multi-chunk** is dominated by the time for reading the input and converting it into a sequence of boundary matrices (displayed in the column “IO”). The compression rate shows the relative file size of the output file in terms of the file size of the input (e.g., 5% means that the input file is 20 times bigger than the

output). We observe that the rate differs over instance classes, but can reduce the chain complex by a factor of more than 10 for many instances. We remark that the output complex might well be bigger even if the total number of generators does not increase because of potential fill-up of the boundary matrices. While this happens for the full function Rips datasets, we point out that passing to this (slightly) larger chain complex is still beneficial for computing minimal presentations, as we demonstrate later in the experiments. Finally, we see a nearly linear behavior in time and memory for all instance classes.

Class	N	Time	IO	Memory	Compression rate
FFR	0.51M	2.39	92%	292MB	132%
	1.00M	5.07	91%	628MB	158%
	2.00M	10.2	91%	1.25GB	160%
	4.02M	22.3	89%	2.72GB	188%
FRT	2M	6.5	96%	1.05GB	23%
	4M	13.7	95%	2.08GB	23%
	8M	28.1	96%	4.17GB	23%
	16M	57.5	96%	8.43GB	23%
PoS	2M	6.18	97%	0.90GB	26%
	4M	12.7	97%	1.74GB	25%
	8M	25.9	97%	3.45GB	26%
	16M	51.5	97%	6.80GB	26%
RDT	2.29M	5.19	95%	1.01GB	1.1%
	4.59M	10.9	93%	1.99GB	1.3%
	9.22M	23.4	91%	3.95GB	1.7%
	18.5M	51.4	86%	7.95GB	2.4%
MCF	2.02M	4.36	95%	0.97GB	6.7%
	4.01M	9.21	95%	1.90GB	7.0%
	8.10M	19.6	95%	3.83GB	7.8%
	16.1M	40.9	95%	7.49GB	8.8%
OFF	0.17M	0.43	96%	80.3MB	23%
	2.38M	5.5	97%	1.00GB	26%
	3.28M	8.39	97%	1.33GB	26%
	5.00M	13.8	97%	2.11GB	24%

Table 2: Results for **multi-chunk** on large datasets. From left to right: class of input, number of generators, running time (in seconds), percentage of running time used for IO operations, memory consumption, and compression rate.

Combining multi-chunk and mpfree On the same instances as in the previous paragraph, we also ran **mpfree**. More precisely we computed all minimal presentations induced by the chain complex, that is, for any pair of consecutive maps, we applied **mpfree** independently. The output is then a sequence of $d - 1$ minimal presentations for a chain complex of length d . We measured both the running time of the sequential and the parallel version of **mpfree**. Table 3 shows

the timings on the left (“mpfree only”). We observe a super-linear behaviour in running time and a close-to-linear behavior in memory for most examples. Also, we can see that parallelization only gives marginal speed-ups, if at all.

Futhermore, we combined both algorithms by first applying `multi-chunk` on the input chain complex and subsequently applying `mpfree` on the compressed chain complex, with the same workflow as above. As we observe in Table 3, the success of preprocessing with `multi-chunk` varies from class to class, but is sometimes significant, in particular for the multi-cover and the random Delaunay data. One aspect is the length of the chain complex: the `multi-chunk` preprocessing can make use of the clearing optimization to avoid many column operations that would otherwise be performed in the subroutines `Min_gens` and `Ker_basis`. But also for short chain complexes where clearing does not apply, `multi-chunk` reduces the time and memory consumption. In particular, the performance of the combined algorithm is coming much closer to a linear behaviour.

The last column of Table 3 shows the compression rate as the ratio of the file sizes of all minimal presentations combined over the size of the input (as before, 5% means that the input file is 20 times bigger than the output). We see that indeed, the minimal presentations are significantly smaller than the input chain complex.

While in the sequential version, `multi-chunk` does not help for full function Rips filtrations (FFR), it still leads to a time improvement with parallelization (at the cost of using more memory). The reason is that most time in these instances is spent on column reductions in the dominant highest dimension and the `multi-chunk` allows for a parallel processing of these steps. It should be remarked, however, that the execution is done with 12 threads, and the speed-up is far away from the ideal factor of 12.

We also report on a perhaps surprising observation. For that, we truncated chain complexes $C_n \rightarrow \dots \rightarrow C_1 \rightarrow C_0 \rightarrow 0$ of length > 2 (classes FRT, RDT, and MCF) to a short chain complex $C_2 \rightarrow C_1 \rightarrow C_0$. The truncated chain complex is smaller in size, saving time on IO operations, and `mpfree` needs to be called only once. Nevertheless, as we see in Table 4, the total running time is still sometimes larger for the truncated chain complex, compared to computing all minimal presentations using `multi-chunk` (compare the RDT instances in Tables 3 and 4). The reason for this slow-down is that for the full chain complex, `multi-chunk` can use the clearing optimization to avoid the reduction of the majority of columns in the first map of the chain complex, whereas this information is lost in the truncated complex, and the algorithm has to fully reduce all columns to zero.

Detailed runtime analysis We list the running time of the major substeps of the algorithm in Table 5. We restrict to the generally best configuration, namely running `multi-chunk` before `mpfree`, with parallelization.

We observe that, similar to running `multi-chunk` alone, a substantial part of the running time goes into reading the input file and building up the matrices,

Class	N	mpfree only				mpfree and multi-chunk				Size
		sequential		parallel		sequential		parallel		
		Time	Memory	Time	Memory	Time	Memory	Time	Memory	
FFR	0.51	2.01	0.32	2.07	0.32	2.1	0.41	1.60	0.42	0.02%
	1.00	4.64	0.63	4.82	0.63	4.89	0.89	3.42	0.92	0.01%
	2.00	9.84	1.24	10.0	1.24	10.1	1.79	7.11	1.83	0.01%
	4.02	24.3	2.49	24.6	2.49	25.2	3.91	16.0	4.02	0.01%
FRT	2	13.0	1.52	12.7	1.62	8.05	1.13	7.51	1.16	9.4%
	4	29.4	2.92	28.7	3.23	17.3	2.21	16.1	2.32	9.4%
	8	65.8	5.98	63.8	6.46	37.6	4.42	35.1	4.61	9.3%
	16	145	12.4	140	13.3	80.7	8.80	74.8	9.23	9.3%
PoS	2	12.6	2.91	11.9	3.55	6.77	1.10	6.48	1.17	0.04%
	4	27.5	6.34	25.8	7.76	14.4	2.19	13.7	2.35	0.03%
	8	60.7	13.9	55.7	17.46	30.4	4.41	28.8	4.76	0.02%
	16	134	30.8	122	39.13	63.7	8.83	60.0	9.76	0.02%
RDT	2.29	25.5	2.35	24.1	2.69	5.92	0.99	5.22	1.01	0.7%
	4.59	69.5	5.11	65.0	5.79	13.9	1.92	11.1	1.99	0.9%
	9.22	191	11.14	176	12.84	35.2	3.81	23.9	3.95	1.2%
	18.5	555	24.63	500	28.93	98.4	7.59	52.6	7.96	1.8%
MCF	2.02	37.8	3.23	36.6	3.68	5.41	0.95	5.1	0.97	3.4%
	4.01	112	7.50	108	8.75	11.7	1.85	10.8	1.91	3.7%
	8.10	330	17.4	317	20.7	26.7	3.77	23.7	3.92	4.3%
	16.1	927	38.0	889	46.2	61.5	7.67	52.6	7.90	5.0%
OFF	0.17	0.87	0.18	0.82	0.20	0.43	0.09	0.41	0.09	0.5%
	2.38	19.4	3.20	18.6	3.73	6.53	1.16	6.13	1.23	0.1%
	3.28	26.0	4.01	24.6	4.63	10.3	1.63	9.69	1.74	0.3%
	5.00	39.0	5.90	37.3	6.81	15.2	2.35	14.3	2.48	0.2%

Table 3: Results for running `mpfree` and combining `mpfree` with `multi-chunk`, sequential and parallel version. From left to right: class of input, number of generators (in millions), running time (in seconds) and memory consumption (in GB) (four times). The last column denotes the total size of all minimal presentation files (in bytes) divided by the size of the input size (also in bytes).

speaking in favor of the efficiency of our algorithm. We observe that depending on the instance, the more expensive steps of the method are the compression subroutine of `multi-chunk`, and the subroutines `Min.Gens` and `Ker.basis` of `mpfree`. Without parallelization, the increase in running time (visible in Table 3) is mostly due to the increased running time of the compression subroutine. When `multi-chunk` is not used, `Min.Gens` and `Ker.basis` get more expensive, resulting in a further increase in runtime. The conference version [18] contains some precise numbers which we omit for brevity.

6 Conclusions

We presented the two compression techniques `multi-chunk` and `mpfree` which preserve homological properties of the underlying data sets with significant compression rates and fast performance.

There is no doubt that compression is an inevitable step in making multi-parameter persistent homology a practical tool for data analysis. We hope that

Class	N	mpfree only				mpfree and multi-chunk			
		sequential		parallel		sequential		parallel	
		Time	Memory	Time	Memory	Time	Memory	Time	Memory
FRT	1.12	6.52	1.01	6.33	1.12	4.50	0.71	4.37	0.74
	2.24	14.9	2.05	14.1	2.30	10.1	1.40	9.62	1.47
	4.48	33.3	4.24	31.5	4.63	22.0	2.80	20.9	2.97
	8.97	72.9	8.92	68.4	9.76	46.9	5.68	43.8	6.05
RDT	1.68	10.8	1.63	9.88	1.82	13.9	0.97	5.68	1.08
	3.37	27.3	3.49	24.0	3.90	45.6	2.19	14.3	2.51
	6.75	70.1	7.46	58.0	8.45	161	5.19	40.7	6.16
	13.5	190	16.3	141	18.7	604	13.2	131	16.2
MCF	1.23	9.99	1.20	9.76	1.33	5.61	0.63	4.52	0.67
	2.44	26.4	2.50	25.9	2.78	13.3	1.26	10.6	1.33
	4.93	70.4	5.91	69.1	6.62	32.5	2.57	25.8	2.77
	9.76	176	13.1	172	14.9	77.3	5.27	60.6	5.74

Table 4: Results for running `mpfree` and combining `mpfree` with `multi-chunk`, sequential and parallel version. Note that the instances here are subsets of the corresponding full chain complexes displayed in Table 3. From left to right: class of input, number of generators (in millions), running time (in seconds) and memory consumption (in GB) (four times).

upcoming algorithmic work on 2-parameter filtrations will report in more detail on the performance gains of compression techniques.

We expect our software to be immediately useful for practioners trying to analyze 2-parameter filtrations. Nevertheless, there are many improvements possible: one idea we have not carried over from the 1-parameter setup is the *dualization* or *cohomology* approach, which suggests inverting the chain complex and proceeding with increasing indices. This has proved to be a successful strategy in particular for Vietoris-Rips complexes [44, 21] but is harder to apply for 2 or more parameters. Recently, a result in this direction has been announced [45] and we hope our speed-ups will be complementary to their approach. Better compression rates and/or performance gains could be achieved for special types of filtrations; for example, a result for multi-parameter flag filtrations has been announced recently [46]. Finally, further gains could be achieved by combination approximation techniques, yielding compressed structures that are not equivalent, but provably close to the input.

References

- [1] G. Carlsson and A. Zomorodian, “The theory of multidimensional persistence,” *Discrete & Computational Geometry*, vol. 42, no. 1, pp. 71–93, 2009.
- [2] M. Lesnick and M. Wright, “Interactive visualization of 2-D persistence modules.” arXiv:1512.00180, 2015.

Class	N	Time	IO	LR	CP	MG	KB	RP	Min
FFR	0.51	1.60	0.88	0.04	0.14	0.30	0.00	0.00	0.00
	1.00	3.42	1.74	0.08	0.37	0.75	0.00	0.00	0.00
	2.00	7.11	3.44	0.15	0.76	1.79	0.00	0.00	0.00
	4.02	16.0	7.00	0.30	1.97	4.70	0.00	0.00	0.00
FRT	2	7.51	5.10	0.12	0.12	0.45	0.56	0.12	0.24
	4	16.1	10.4	0.27	0.24	1.12	1.44	0.26	0.56
	8	35.1	21.8	0.51	0.45	2.78	3.69	0.55	1.36
	16	74.8	44.7	1.03	0.91	6.87	8.97	1.13	3.26
PoS	2	6.48	4.62	0.05	0.12	0.17	0.98	0.04	0.02
	4	13.7	9.56	0.10	0.23	0.46	2.26	0.10	0.04
	8	28.8	19.5	0.20	0.43	1.28	5.16	0.20	0.10
	16	60.0	39.2	0.39	0.85	4.02	11.6	0.42	0.23
RDT	2.29	5.22	4.64	0.09	0.14	0.03	0.03	0.02	0.02
	4.59	11.1	9.67	0.19	0.46	0.06	0.07	0.03	0.04
	9.22	23.9	20.3	0.38	1.60	0.16	0.18	0.09	0.10
	18.5	52.6	42.2	0.77	5.97	0.39	0.43	0.23	0.28
MCF	2.02	5.1	3.98	0.10	0.10	0.19	0.29	0.07	0.07
	4.01	10.8	8.23	0.19	0.22	0.47	0.75	0.16	0.18
	8.10	23.7	17.4	0.36	0.49	1.27	2.11	0.36	0.47
	16.1	52.6	36.5	0.74	1.14	3.46	6.11	0.86	1.14
OFF	0.17	0.41	0.32	0.00	0.01	0.00	0.04	0.00	0.00
	2.38	6.13	4.08	0.05	0.10	0.15	1.30	0.05	0.02
	3.28	9.69	6.35	0.08	0.16	0.29	2.09	0.08	0.04
	5.00	14.3	10.4	0.12	0.27	0.27	2.15	0.05	0.04

Table 5: Results for running **multi-chunk** and **mpfree**, parallel version. From left to right: class of input, number of generators (in millions), running time (in seconds), time for IO operations (IO), time for local reductions in **multi-chunk** (LR), time for compression in **multi-chunk** (CP), time for **Min-gens** in **mpfree** (MG), time for **ker.basis** (KB), time for reparameterization (RP), time for minimization (Min)

- [3] M. Kerber, M. Lesnick, and S. Oudot, “Exact computation of the matching distance on 2-parameter persistence modules,” in *35th International Symposium on Computational Geometry (SoCG 2019)*, pp. 46:1–46:15, 2019.
- [4] M. Kerber and A. Nigmetov, “Efficient approximation of the matching distance for 2-parameter persistence,” in *36th International Symposium on Computational Geometry (SoCG 2020)*, 2020.
- [5] H. B. Bjerkevik and M. Kerber, “Asymptotic improvements on the exact matching distance for 2-parameter persistence.” arXiv:2111.10303, 2021.
- [6] T. Dey and C. Xin, “Computing bottleneck distance for 2-D interval decomposable modules,” in *34th International Symposium on Computational*

Geometry (SoCG 2018), pp. 32:1–32:15, 2018.

- [7] R. Corbet, U. Fugacci, M. Kerber, C. Landi, and B. Wang, “A kernel for multi-parameter persistent homology,” *Computers & Graphics: X*, vol. 2, p. 100005, 2019.
- [8] O. Vipond, “Multiparameter persistence landscapes,” *Journal of Machine Learning Research*, vol. 21, no. 61, pp. 1–38, 2020.
- [9] T. Dey and C. Xin, “Generalized persistence algorithm for decomposing multi-parameter persistence modules.” arXiv:1904.03766, 2019.
- [10] M. Kerber, D. Morozov, and A. Nigmetov, “Geometry helps to compare persistence diagrams,” *Journal of Experimental Algorithms*, vol. 22, pp. 1.4:1–1.4:20, Sept. 2017.
- [11] U. Bauer, M. Kerber, and J. Reininghaus, “Clear and compress: Computing persistent homology in chunks,” in *Topological Methods in Data Analysis and Visualization III*, Mathematics and Visualization, pp. 103–117, Springer, 2014.
- [12] M. Lesnick and M. Wright, “Computing minimal presentations and bigraded Betti numbers of 2-parameter persistent homology.” arXiv:1902.05708, 2019.
- [13] M. Kerber, “multi-chunk implementation.” https://bitbucket.org/mkerber/multi_chunk/, 2021.
- [14] M. Kerber and A. Rolle, “mpfree implementation.” <https://bitbucket.org/mkerber/mpfree/>, 2020.
- [15] The RIVET Developers, “RIVET.” 1.1.0, 2020.
- [16] C. Chen and M. Kerber, “Persistent homology computation with a twist,” in *European Workshop on Computational Geometry (EuroCG)*, pp. 197–200, 2011.
- [17] U. Fugacci and M. Kerber, “Chunk reduction for multi-parameter persistent homology,” in *35th International Symposium on Computational Geometry, SoCG 2019*, pp. 37:1–37:14, 2019.
- [18] M. Kerber and A. Rolle, “Fast minimal presentations of bi-graded persistence modules,” in *2021 Proceedings of the Workshop on Algorithm Engineering and Experiments (ALENEX)*, pp. 207–220, SIAM, 2021.
- [19] D. Günther, J. Reininghaus, H. Wagner, and I. Hotz, “Efficient computation of 3D Morse–Smale complexes and persistent homology using discrete Morse theory,” *The Visual Computer*, vol. 28, no. 10, pp. 959–969, 2012.

- [20] K. Mischaikow and V. Nanda, “Morse theory for filtrations and efficient computation of persistent homology,” *Discrete & Computational Geometry*, vol. 50, no. 2, pp. 330–353, 2013.
- [21] U. Bauer, “Ripser: efficient computation of Vietoris–Rips persistence barcodes.” arxiv 1908.02518, 2019.
- [22] A. Hylton, G. Henselman-Petrusek, J. Sang, and R. Short, “Tuning the performance of a computational persistent homology package,” *Softw. Pract. Exp.*, vol. 49, no. 5, pp. 885–905, 2019.
- [23] J. Boissonnat, S. Pritam, and D. Pareek, “Strong collapse for persistence,” in *26th Annual European Symposium on Algorithms, ESA 2018*, pp. 67:1–67:13, 2018.
- [24] J. Boissonnat and S. Pritam, “Edge collapse and persistence of flag complexes,” in *36th International Symposium on Computational Geometry (SoCG 2020)*, pp. 19:1–19:15, 2020.
- [25] D. Sheehy, “Linear-size approximation to the Vietoris–Rips filtration,” *Discrete & Computational Geometry*, vol. 49, pp. 778–796, 2013.
- [26] T. Dey, F. Fan, and Y. Wang, “Computing topological persistence for simplicial maps,” in *ACM Symposium on Computational Geometry (SOCG)*, p. 345, 2014.
- [27] M. Botnan and G. Spreemann, “Approximating persistent homology in Euclidean space through collapses,” *Applied Algebra in Engineering, Communication and Computing*, vol. 26, no. 1-2, pp. 73–101, 2015.
- [28] A. Choudhary, M. Kerber, and S. Raghvendra, “Polynomial-sized topological approximations using the permutahedron,” *Discret. Comput. Geom.*, vol. 61, no. 1, pp. 42–80, 2019.
- [29] A. Choudhary, M. Kerber, and S. Raghvendra, “Improved topological approximations by digitization,” in *Proceedings of the Thirtieth Annual ACM-SIAM Symposium on Discrete Algorithms, SODA 2019, San Diego, California, USA, January 6-9, 2019* (T. M. Chan, ed.), pp. 2675–2688, SIAM, 2019.
- [30] M. Buchet, F. Chazal, S. Y. Oudot, and D. R. Sheehy, “Efficient and robust persistent homology for measures,” *Comput. Geom.*, vol. 58, pp. 70–96, 2016.
- [31] T. Dey, D. Shi, and Y. Wang, “Simba: An efficient tool for approximating Rips-filtration persistence via simplicial batch-collapse,” in *European Symposium on Algorithms (ESA)*, 2016.
- [32] B. Brehm and H. Hardering, “Sparips.” arXiv:1807.09982, 2018.

- [33] M. Allili, T. Kaczynski, and C. Landi, “Reducing complexes in multidimensional persistent homology theory,” *J. Symb. Comput.*, vol. 78, pp. 61–75, 2017.
- [34] M. Allili, T. Kaczynski, C. Landi, and F. Masoni, “Acyclic partial matchings for multidimensional persistence: Algorithm and combinatorial interpretation,” *Journal of Mathematical Imaging and Vision*, pp. 1–19, 2018.
- [35] S. Scaramuccia, F. Iuricich, L. De Floriani, and C. Landi, “Computing multiparameter persistent homology through a discrete Morse-based approach.” arXiv:1811.05396, 2018.
- [36] F. Iuricich, S. Scaramuccia, C. Landi, and L. De Floriani, “A discrete Morse-based approach to multivariate data analysis,” in *SIGGRAPH ASIA 2016 Symposium on Visualization*, p. 5, ACM, 2016.
- [37] M. Kashiwara and P. Schapira, *Categories and Sheaves*. Grundlehren der mathematischen Wissenschaften, Springer-Verlag Berlin Heidelberg, 2006.
- [38] D. Eisenbud, *Commutative Algebra: With a View Toward Algebraic Geometry*. Graduate Texts in Mathematics, Springer, 1995.
- [39] M. Kerber and M. Lesnick, “scc2020: A file format for sparse chain complexes in TDA.” available at https://bitbucket.org/mkerber/chain_complex_format/, 2021.
- [40] U. Fugacci, M. Kerber, and A. Rolle, “Benchmark dataset for compression for 2-parameter persistent homology.” TU Graz Repository, 2022. <https://doi.org/10.3217/xcs8c-hjm53>.
- [41] C. Jamin, S. Pion, and M. Teillaud, “3D triangulations,” in *CGAL User and Reference Manual*, CGAL Editorial Board, 5.0.3 ed., 2020.
- [42] R. Corbet, M. Kerber, M. Lesnick, and G. Osang, “Computing the multicover bifiltration,” in *37th International Symposium on Computational Geometry, SoCG 2021*, vol. 189 of *LIPICs*, pp. 27:1–27:17, 2021.
- [43] H. Edelsbrunner and G. Osang, “The multi-cover persistence of euclidean balls,” in *34th International Symposium on Computational Geometry, SoCG 2018*, vol. 99 of *LIPICs*, pp. 34:1–34:14, 2018.
- [44] U. Bauer, M. Kerber, J. Reininghaus, and H. Wagner, “Phat - persistent homology algorithms toolbox,” *Journal of Symbolic Computation*, vol. 78, pp. 76–90, 2017.
- [45] F. Lenzen, U. Bauer, and M. Lesnick, “Efficient two-parameter persistence computation via cohomology,” in *Computational Geometry: Young Researchers Forum 2021*, LIPICs, 2021.

- [46] Á. J. Alonso, M. Kerber, and S. Pritam, “Reducing multi-parameter flag filtrations via edge collapses,” in *Computational Geometry: Young Researchers Forum 2022*, LIPICS, 2022.
- [47] H. Edelsbrunner and J. Harer, *Computational topology: an introduction*. American Mathematical Society, 2010.

A Detailed proofs

We begin by completing the proof of Theorem 3.2.

Proposition A.1. *The maps r^\bullet and s^\bullet are homotopy-inverse one with respect to the other.*

Proof. Let us define a collection of maps $\phi^l : F^l \rightarrow F^{l+1}$, for any $l \in \mathbb{N}$. Given $c \in B^l$, the map ϕ^l is defined as:

$$\phi^l(c) = \begin{cases} \langle c, c_1 \rangle c_2 & \text{if } l = n, \\ 0 & \text{otherwise.} \end{cases}$$

The result follows from the following facts, which are straightforward to check. For any l :

- (1) $s^l r^l$ is chain-homotopic to id_{F^l} via ϕ^l ,
- (2) $r^l s^l = \text{id}_{F^l}$.

□

We now complete the proofs of the results of Section 3.5. Let A^\bullet, B^\bullet be two chain complexes such that A^\bullet is a subcomplex of B^\bullet and let $\eta^n : H^n(A^\bullet) \rightarrow H^n(B^\bullet)$ be the map in homology induced by this inclusion. Let us consider the boundary matrix of B^\bullet in which the generators of A^\bullet are placed on the left with respect to the generators of B^\bullet not belonging to A^\bullet . By applying the standard reduction algorithm for computing persistent homology [47], we obtain a reduced matrix R . To avoid a clash in terminology with previous parts of the paper, we refer to the entry of lowest position in the matrix among the non-zero ones in column c' as the *lowest index* of c' . Let us denote the columns of R corresponding to the generators of B^\bullet not belonging to A^\bullet as the columns of $B^\bullet \setminus A^\bullet$ and the others as the columns of A^\bullet .

Lemma A.2. *We have that:*

- the number of the n -columns of $B^\bullet \setminus A^\bullet$ having as lowest index a column of A^\bullet is equal to $\dim \text{Ker } \eta^{n-1}$,
- the number of the n -columns of $B^\bullet \setminus A^\bullet$ with null boundary for which there is no column in R having them as lowest index is equal to $\dim \text{Coker } \eta^n$.

Proof. We can partition the n -columns of $B^\bullet \setminus A^\bullet$ in three distinct classes. The first class includes the n -columns of $B^\bullet \setminus A^\bullet$ having as lowest index a column of A^\bullet . According to the standard reduction algorithm, these columns are in one-to-one correspondence with the non-zero homology classes of $H^{n-1}(A^\bullet)$ that become trivial in $H^{n-1}(B^\bullet)$. So, their number coincides with the dimension of $\text{Ker } \eta^{n-1}$. The second class includes the n -columns of $B^\bullet \setminus A^\bullet$ with null boundary for which there is no column in R having them as lowest index. According to the standard reduction algorithm, these columns are in one-to-one correspondence with the homology classes that are born in $H^n(B^\bullet)$. So, their number coincides with the dimension of $\text{Coker } \eta^n$. The third class of n -columns of $B^\bullet \setminus A^\bullet$ are the ones with lowest index in $B^\bullet \setminus A^\bullet$ or the columns with null boundary which are the lowest index of a column of $B^\bullet \setminus A^\bullet$. \square

Theorem A.3. *Let G^\bullet be the output of `multi-chunk` applied to the input F^\bullet . Then $\delta_p^n(F^\bullet) = \gamma_p^n(G^\bullet)$.*

Proof. Let us apply Lemma A.2 to the case $A^\bullet = F_{<\mathbf{p}}^\bullet$ and $B^\bullet = F_{\mathbf{p}}^\bullet$. Note that the local reduction phase at grade \mathbf{p} in `multi-chunk` corresponds to a partial reduction of the matrix of $F_{\mathbf{p}}^\bullet$, because all column additions are left-to-right, and it is known that the lowest indices of the reduced matrix are invariant under left-to-right column additions. At the end of the local reduction phase, each column is labeled as local (positive or negative), or global. A local column is paired with another local column of grade \mathbf{p} , and this pairing will not change when completing the partial reduction to a completely reduced matrix for $F_{\mathbf{p}}^\bullet$. The reason is simply that all columns in $F_{<\mathbf{p}}^\bullet$ have a lowest index with smaller index than any column of grade \mathbf{p} . By the above reasoning, the local columns will neither contribute to kernel nor cokernel of $\eta_{\mathbf{p}}^{n-1}$.

On the other hand, consider a global column with grade \mathbf{p} . Its lowest index corresponds to a column in $F_{<\mathbf{p}}^\bullet$ after the local reduction phase. Since the lowest index can only decrease when further reducing the matrix, it follows that in the reduced matrix, the global column has still a lowest index in $F_{<\mathbf{p}}^\bullet$, in which case it contributes to $\text{Ker } \eta_{\mathbf{p}}^{n-1}$, or its boundary becomes null. In the latter case, it cannot be paired with another column at grade \mathbf{p} since then, this pairing would have been identified already at the local reduction phase. Hence, the global column contributes to $\text{Coker } \eta_{\mathbf{p}}^n$. After all, each global column contributes to the kernel or the cokernel, and therefore, the number of global columns is equal to $\delta_p^n(F^\bullet)$. Moreover, the number of global columns at grade \mathbf{p} is exactly the number of generators added at grade \mathbf{p} to the output complex G^\bullet . \square

Now, let \bar{F}^\bullet be any chain complex of finitely generated free persistence modules. Since each n -generator newly introduced in $\bar{F}_{\mathbf{p}}^\bullet$ can act on the homology by just increasing the dimension of $\text{Ker } \eta_{\mathbf{p}}^{n-1}$, or alternatively of $\text{Coker } \eta_{\mathbf{p}}^n$, at most by 1, we have that

$$\delta_p^n(\bar{F}^\bullet) = \dim \text{Ker } \eta_{\mathbf{p}}^{n-1} + \dim \text{Coker } \eta_{\mathbf{p}}^n \leq \dim \bar{F}_{\mathbf{p}}^n - \dim \bar{F}_{<\mathbf{p}}^n = \gamma_p^n(\bar{F}^\bullet). \quad (1)$$

Theorem A.4. *Any chain complex of free persistence modules \bar{F}^\bullet quasi-isomorphic to F^\bullet has to add at least $\delta_p^n(F^\bullet)$ n -generators at grade \mathbf{p} . I.e., $\delta_p^n(F^\bullet) \leq \gamma_p^n(\bar{F}^\bullet)$.*

Proof. Let $f^\bullet : F^\bullet \rightarrow \bar{F}^\bullet$ be the quasi-isomorphism between F^\bullet and \bar{F}^\bullet . Thanks to their commutativity with the inclusion maps, we have an induced chain map $f_{<\mathbf{p}}^\bullet : F_{<\mathbf{p}}^\bullet \rightarrow \bar{F}_{<\mathbf{p}}^\bullet$. This ensures for any $\mathbf{p} \in \mathbb{Z}^2$, the construction of the following commutative diagram

$$\begin{array}{ccccccccc} 0 & \longrightarrow & F_{\mathbf{p}_0}^n & \longrightarrow & F_{\mathbf{p}_1}^n \oplus F_{\mathbf{p}_2}^n & \longrightarrow & F_{<\mathbf{p}}^n & \longrightarrow & 0 \\ & & \downarrow f_{\mathbf{p}_0}^n & & \downarrow (f_{\mathbf{p}_1}^n, f_{\mathbf{p}_2}^n) & & \downarrow f_{<\mathbf{p}}^n & & \\ 0 & \longrightarrow & \bar{F}_{\mathbf{p}_0}^n & \longrightarrow & \bar{F}_{\mathbf{p}_1}^n \oplus \bar{F}_{\mathbf{p}_2}^n & \longrightarrow & \bar{F}_{<\mathbf{p}}^n & \longrightarrow & 0 \end{array}$$

in which each row is exact. Thanks to the quasi-isomorphism established by f and to the Mayer-Vietoris sequence, we can derive from the previous one the following commutative diagram

$$\begin{array}{ccccccccc} H^n(F_{\mathbf{p}_0}^\bullet) & \longrightarrow & H^n(F_{\mathbf{p}_1}^\bullet) \oplus H^n(F_{\mathbf{p}_2}^\bullet) & \longrightarrow & H^n(F_{<\mathbf{p}}^\bullet) & \longrightarrow & H^{n-1}(F_{\mathbf{p}_0}^\bullet) & \longrightarrow & H^{n-1}(F_{\mathbf{p}_1}^\bullet) \oplus H^{n-1}(F_{\mathbf{p}_2}^\bullet) \\ \downarrow \psi_{\mathbf{p}_0}^n & & \downarrow (\psi_{\mathbf{p}_1}^n, \psi_{\mathbf{p}_2}^n) & & \downarrow \psi_{<\mathbf{p}}^n & & \downarrow \psi_{\mathbf{p}_0}^{n-1} & & \downarrow (\psi_{\mathbf{p}_1}^{n-1}, \psi_{\mathbf{p}_2}^{n-1}) \\ H^n(\bar{F}_{\mathbf{p}_0}^\bullet) & \longrightarrow & H^n(\bar{F}_{\mathbf{p}_1}^\bullet) \oplus H^n(\bar{F}_{\mathbf{p}_2}^\bullet) & \longrightarrow & H^n(\bar{F}_{<\mathbf{p}}^\bullet) & \longrightarrow & H^{n-1}(\bar{F}_{\mathbf{p}_0}^\bullet) & \longrightarrow & H^{n-1}(\bar{F}_{\mathbf{p}_1}^\bullet) \oplus H^{n-1}(\bar{F}_{\mathbf{p}_2}^\bullet) \end{array}$$

in which each row is exact and the horizontal and the vertical maps are induced by the corresponding ones between chain complexes. Since all the other four vertical maps are isomorphisms, the 5-lemma ensures that map $\psi_{<\mathbf{p}}^n$ is also an isomorphism. So, we have the following commutative diagram

$$\begin{array}{ccc} H^n(F_{<\mathbf{p}}^\bullet) & \xrightarrow{\iota_{\mathbf{p}}^n} & H^n(F_{\mathbf{p}}^\bullet) \\ \psi_{<\mathbf{p}}^n \downarrow & & \downarrow \psi_{\mathbf{p}}^n \\ H^n(\bar{F}_{<\mathbf{p}}^\bullet) & \xrightarrow{\eta_{\mathbf{p}}^n} & H^n(\bar{F}_{\mathbf{p}}^\bullet) \end{array}$$

in which vertical maps are isomorphisms. Then, for any n , $\dim \text{Ker } \eta_{\mathbf{p}}^n = \dim \text{Ker } \iota_{\mathbf{p}}^n$ and $\dim \text{Coker } \eta_{\mathbf{p}}^n = \dim \text{Coker } \iota_{\mathbf{p}}^n$. So, by applying Equation (1), we have that

$$\begin{aligned} \delta_{\mathbf{p}}^n(F^\bullet) &= \dim \text{Ker } \iota_{\mathbf{p}}^{n-1} + \dim \text{Coker } \iota_{\mathbf{p}}^n = \dim \text{Ker } \eta_{\mathbf{p}}^{n-1} + \dim \text{Coker } \eta_{\mathbf{p}}^n \\ &\leq \dim \bar{F}_{\mathbf{p}}^n - \dim \bar{F}_{<\mathbf{p}}^n = \gamma_{\mathbf{p}}^n(\bar{F}^\bullet). \end{aligned}$$

□

B Pseudocode

In this section, we give pseudocode for some of the algorithms discussed in the paper. Algorithm 1 describes the locality test, while Algorithms 2, 3, and 4

describe the three phases (local reduction, compression, and removal of local columns) of **multi-chunk**. Algorithms 5–9 describe the subroutines of the LW algorithm, and Algorithms 10–12 describe our improved versions. We mark the for loops in the pseudocode that can be run in parallel.

Algorithm 1 Locality test

```

function IS_LOCAL( $A, i$ )
  if column  $i$  in  $A$  is 0 then
    return true
  end if
   $j \leftarrow$  pivot of column  $i$  in  $A$ 
  Return true iff the column grade of  $i$  in  $A$  equals the row grade of  $j$  in  $A$ 
end function

```

Algorithm 2 Local reduction

```

function LOCAL_REDUCTION( $A, LocPos, LocNeg, Global$ )
   $\triangleright A$ , a graded boundary matrix  $[\partial^n]^{B^n, B^{n-1}}$  of a chain complex  $F^\bullet$ 
   $\triangleright LocPos, LocNeg, Global$ , subsets of the generators of  $F^\bullet$ 
  for  $c$  column of  $A$  and not in  $LocPos \cup LocNeg \cup Global$  do
     $\triangleright$  Columns are traversed in increasing order w.r.t. index  $i$ 
    while IS_LOCAL( $A, c$ ) and  $\exists c'$  column of  $A$  with  $i(c') < i(c)$  do
       $c \leftarrow c + c'$ 
    end while
    if IS_LOCAL( $A, c$ ) then
      Add  $c$  to  $LocNeg$ 
      Add the local pivot  $c'$  of  $c$  to  $LocPos$ 
    else
      Add  $c$  to  $Global$ 
    end if
  end for
  return  $LocPos, LocNeg, Global$ 
end function

```

Algorithm 3 Compression

```
function COMPRESSION( $A, LocPos, LocNeg, Global$ )  
   $\triangleright A$ , a graded boundary matrix  $[\partial^n]^{B^n, B^{n-1}}$  of a chain complex  $F^\bullet$   
   $\triangleright LocPos, LocNeg, Global$ , subsets of the generators of  $F^\bullet$   
  for  $c$  column of  $A$  and in  $Global$  do  
    while boundary of  $c$  contains an elements of  $LocNeg \cup LocPos$  do  
      Pick local generator  $c'$  in the boundary of  $c$  with maximal index  
      if  $c' \in LocNeg$  then  
        Remove  $c'$  from the boundary of  $c$   
      else  $\triangleright c' \in LocPos$   
        Denote as  $c''$  the  $n$ -column in  $LocNeg$  with  $c'$  as local pivot  
         $c \leftarrow c + c''$   
      end if  
    end while  
  end for  
  return  $A$   
end function
```

Algorithm 4 Removal of local pairs

```
function LOCAL_PAIRS_REMOVAL( $A, LocPos, LocNeg, Global$ )  
   $\triangleright A$ , a graded boundary matrix  $[\partial^n]^{B^n, B^{n-1}}$  of a chain complex  $F^\bullet$   
   $\triangleright LocPos, LocNeg, Global$ , subsets of the generators of  $F^\bullet$   
  for  $c$  column of  $A$  do  
    if  $c \in LocNeg \cup LocPos$  then  
      Remove  $c$  from  $A$   
    end if  
  end for  
  for  $r$  row of  $A$  do  
    if  $r \in LocNeg \cup LocPos$  then  
      Remove  $r$  from  $A$   
    end if  
  end for  
  return  $A$   
end function
```

Algorithm 5 Matrix reduction, LW-version

```
function REDUCE_LW( $A, j, use\_auxiliary = false$ )  
   $\triangleright A$  maintains a pivot vector  $piv$   
   $\triangleright piv[i] = k$  means that column  $k$  in  $A$  has pivot  $i$ .  
   $\triangleright piv[i] = -1$  means that no (visited) column in  $A$  has pivot  $i$ .  
   $\triangleright$  If  $use\_auxiliary$  is set,  $A$  also maintains an auxiliary matrix.  
  while column  $j$  in  $A$  is not empty do  
     $i \leftarrow$  pivot of column  $j$   
     $k \leftarrow piv[i]$   
    if  $k = -1$  or  $k > j$  then  
       $piv[i] \leftarrow j$   
      break  
    else  
      add column  $k$  to column  $j$   
      if  $use\_auxiliary$  then  
        add auxiliary-column  $k$  to auxiliary-column  $j$   
      end if  
    end if  
  end while  
end function
```

Algorithm 6 Min_gens, LW-version

```
function MIN_GENS_LW( $A$ )  
   $(X, Y) \leftarrow grid\_dim\_of(A)$   $\triangleright$  grades of  $A$  are on  $X \times Y$  grid  
   $Out \leftarrow \emptyset$   
  for  $x = 1, \dots, X$  do  
    for  $y = 1, \dots, Y$  do  
       $L \leftarrow$  column indices of  $A$  with grades  $(0, y), \dots, (x-1, y)$  in order  
      for  $i \in L$  do  
        REDUCE_LW( $A, i$ )  
      end for  
       $I \leftarrow$  column indices of  $A$  with grade  $(x, y)$   
      for  $i \in I$  do  
        REDUCE_LW( $A, i$ )  
        if column  $i$  is not zero then  
          Append column  $i$  to  $Out$  with grade  $(x, y)$   
        end if  
      end for  
    end for  
  end for  
  return  $Out$   
end function
```

Algorithm 7 Ker.basis, LW-version

```
function KER_BASIS_LW( $B$ )
  ( $X, Y$ )  $\leftarrow$  grid_dim_of( $B$ )            $\triangleright$  grades of  $B$  are on  $X \times Y$  grid
   $Out \leftarrow \emptyset$ 
  for  $x = 1, \dots, X$  do
    for  $y = 1, \dots, Y$  do
       $L \leftarrow$  column indices of  $B$  with grades  $(0, y), \dots, (x, y)$  in order
      for  $i \in L$  do
        REDUCE_LW( $B, i, use\_auxiliary = true$ )
        if column  $i$  has turned from non-zero to zero then
          Append auxiliary-column of  $i$  to  $Out$  with grade  $(x, y)$ 
        end if
      end for
    end for
  end for
  return  $Out$ 
end function
```

Algorithm 8 Reparameterize

```
function REPARAM( $G, K$ )
   $\triangleright G$  is the output of MIN_GENs( $A$ )
   $\triangleright K$  is the output of KER_BASIS( $B$ )
  Form matrix  $(K|G)$  by concatenation.
   $Out \leftarrow \emptyset$ 
  for  $i$  in index range of  $G$ -column in  $(K|G)$  do            $\triangleright$  Parallelizable
    REDUCE_LW( $(K|G), i, use\_auxiliary = true$ )            $\triangleright$  Column  $i$  is zero
  afterwards
    Append the auxiliary column  $i$  to  $Out$ 
  end for
  return  $Out$ 
end function
```

Algorithm 9 Minimization, LW-version

```
function MINIMIZE_LW( $M'$ )  
   $n \leftarrow \#$  columns in  $M'$   
  for  $i = 1, \dots, n$  do  
    if IS_LOCAL( $M', i$ ) then  
       $j \leftarrow$  pivot of column  $i$  in  $M'$   
      for  $k = i + 1, \dots, n$  do  
        if column  $k$  in  $M'$  contains  $j$  as row index then  
          Add column  $i$  to column  $k$   
        end if  
      end for  
      Mark column  $i$  and row  $j$  in  $M'$   
    end if  
  end for  
   $M \leftarrow$  submatrix of  $M'$  consisting of unmarked rows and columns  
  Re-index the columns of  $M$  and return  $M$   
end function
```

Algorithm 10 Matrix reduction, new version

function REDUCE_NEW($A, i, grade, use_auxiliary = false, local_check = false$)

- ▷ $grade$ is the grade that the algorithm is currently considering
- ▷ On top of pivot vector and auxiliary vector, A maintains priority queues:
- ▷ $cols_at_y_grade[y_0]$ is a priority queue for column indices at y -grade y_0
- ▷ $grade_queue$ is a priority queue of grades that the algorithm needs to look at

while column i in A is not empty **do**
 $j \leftarrow$ pivot of column i
 $k \leftarrow piv[j]$
 if $k = -1$ **then**
 $piv[j] \leftarrow i$
 break
 end if
 if $k > j$ **then**
 $y \leftarrow$ y -grade of column k in A
 Push k to $cols_at_y_grade[y]$
 $x \leftarrow$ x -grade of $grade$
 Push (x, y) to $grade_queue$
 $piv[j] \leftarrow i$
 break
 end if
 if $local_check$ and not IS_LOCAL(A, i) **then**
 break
 end if
 add column k to column i
 if $use_auxiliary$ **then**
 add auxiliary-column k to auxiliary-column i
 end if
end while
end function

Algorithm 11 Min_gens, new version

```
function MIN_GENS_NEW( $A$ )
  Initialize  $grade\_queue$  as empty priority queue
  for each column  $c$  of  $A$  do
    Push the grade of  $c$  into  $grade\_queue$ 
  end for
  for each  $y$ -grade  $y_0$  that appears in a column of  $A$  do
    Initialize  $cols\_at\_y\_grade[y_0]$  as empty priority queue
  end for
   $Out \leftarrow \emptyset$ 
  while  $grade\_queue$  is not empty do
    Pop the grade  $(x, y)$  from  $grade\_queue$  minimal in lex order
    Push all column indices at grade  $(x, y)$  into  $cols\_at\_y\_grade[y]$ 
    while  $cols\_at\_y\_grade[y]$  is not empty do
      Pop column index  $i$  from  $cols\_at\_y\_grade[y]$  minimal in lex order
      REDUCE_NEW( $A, i, (x, y)$ )     $\triangleright$  Might change the priority queues as
side effect
      if column  $i$  is not 0 and its grade is  $(x, y)$  then
        Append column  $i$  to  $Out$  with grade  $(x, y)$ 
      end if
    end while
  end while
  return  $Out$ 
end function
```

Algorithm 12 Ker.basis, new version

```
function KER_BASIS_NEW( $B$ )
  Initialize  $grade\_queue$  as empty priority queue
  for each column  $c$  of  $B$  do
    Push the grade of  $c$  into  $grade\_queue$ 
  end for
  for each  $y$ -grade  $y_0$  that appears in a column of  $B$  do
    Initialize  $cols\_at\_y\_grade[y_0]$  as empty priority queue
  end for
   $Out \leftarrow \emptyset$ 
  while  $grade\_queue$  is not empty do
    Pop the grade  $(x, y)$  from  $grade\_queue$  minimal in lex order
    Push all column indices at grade  $(x, y)$  into  $cols\_at\_y\_grade[y]$ 
    while  $cols\_at\_y\_grade[y]$  is not empty do
      Pop column index  $i$  from  $cols\_at\_y\_grade[y]$  minimal in lex order
      REDUCE_NEW( $B, i, (x, y), use\_auxiliary=true$ )  $\triangleright$  Might change the
      priority queues as side effect
      if column  $i$  has turned from non-zero to zero then
        Append auxiliary-column  $i$  to  $Out$  with grade  $(x, y)$ 
      end if
    end while
  end while
  return  $Out$ 
end function
```
